Environmental Science & Technology

Article

Cite This: Environ. Sci. Technol. 2017, 51, 14217−14224

pubs.acs.org/est

UV/Peracetic Acid for Degradation of Pharmaceuticals and Reactive Species Evaluation

Meiquan Cai,[†,‡,§] Peizhe Sun,[‡,∥] Liqiu Zhang,*[,†] and Ching-Hua Huang*[,‡]

[†]College of Environmental Science and Engineering, Beijing Forestry University, Beijing 100083, P. R. China

[‡]School of Civil and Environmental Engineering, Georgia Institute of Technology, Atlanta, Georgia 30332, United States

[§]School of Environment, Tsinghua University, Beijing 100084, P. R. China

[∥]School of Environmental Science and Engineering, Tianjin University, Tianjin 30072, P. R. China

Supporting Information

ABSTRACT: Peracetic acid (PAA) is a widely used disinfectant, and combined UV light with PAA (i.e., UV/PAA) can be a novel advanced oxidation process for elimination of water contaminants. This study is among the first to evaluate the photolysis of PAA under UV irradiation (254 nm) and degradation of pharmaceuticals by UV/PAA. PAA exhibited high quantum yields ($\Phi_{254\ nm}$ = 1.20 and 2.09 mol·Einstein^{-1} for the neutral (PAA^0) and anionic (PAA^-) species, respectively) and also showed scavenging effects on hydroxyl radicals ($k_{^\bullet OH/PAA^0}$ = (9.33 ± 0.3) × 10^8 $M^{-1}\cdot s^{-1}$ and $k_{^\bullet OH/PAA^-}$ = (9.97 ± 2.3) × 10^9 $M^{-1}\cdot s^{-1}$). The pharmaceuticals were persistent with PAA alone but degraded rapidly by UV/PAA. The contributions of direct photolysis, hydroxyl radicals, and other radicals to pharmaceutical degradation under UV/PAA were systematically evaluated. Results revealed that •OH was the primary radical responsible for the degradation of carbamazepine and ibuprofen by UV/PAA, whereas $CH_3C(=O)O^\bullet$ and/or $CH_3C(=O)O_2^\bullet$ contributed significantly to the degradation of naproxen and 2-naphthoxyacetic acid by UV/PAA in addition to •OH. The carbon-centered radicals generated from UV/PAA showed strong reactivity to oxidize certain naphthyl compounds. The new knowledge obtained in this study will facilitate further research and development of UV/PAA as a new degradation strategy for water contaminants.

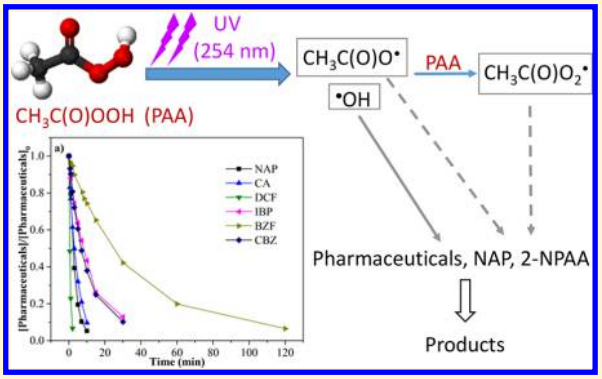

INTRODUCTION

Peracetic acid (PAA, $CH_3C(=O)OOH$) is an organic peroxy acid known as a broad-spectrum antimicrobial agent.[1,2] Commercial PAA solutions, synthesized by acid-catalyzed reaction of hydrogen peroxide (H_2O_2) with acetic acid ($CH_3C(=O)OH$), are typically a mixture of PAA, H_2O_2, $CH_3C(=O)OH$, and water.[3] The oxidation potential of PAA is higher than that of H_2O_2 (1.96 vs 1.78 eV),[4] and the antimicrobial effect of PAA is far greater than H_2O_2, although synergistic effects of PAA and H_2O_2 in commercial PAA solution for inactivation of bacteria were also reported.[1,2,5,6] The undissociated species of PAA (PAA^0) at pH less than 8.2 ($pK_{a,PAA}$, 25 °C)[7] is considered to be the biocidal form instead of the dissociated species (PAA^-).[8]

Owing to the advantages of high sterilization ability, limited toxic byproduct formation, and easy retrofit, PAA is widely applied in food, medical, and textile industries and is used for wastewater disinfection in the U.S., Canada, and Europe.[1,9−14] Since the USEPA considered the use of PAA as an alternative for combined sewer overflow and wastewater disinfection, the application of PAA in wastewater treatment has received increasing attention.[15,16] Furthermore, PAA was found to be more effective than NaOCl in controlling enteric microorganisms.[17] Thus, PAA may become more common to replace NaOCl in wastewater disinfection in the future.

With more wastewater treatment plants to employ PAA for disinfection, the potential of PAA to degrade micropollutants merits more study. Previous research observed that PAA was a good oxidant for removing 4-chlorophenol, but others found PAA ineffective for degrading certain pharmaceuticals (e.g., ibuprofen, naproxen, diclofenac, gemfibrozil, and clofibric acid) in sewage effluents.[18,19] Some have investigated the combination of UV light and PAA (i.e., UV/PAA) for wastewater disinfection, and reported synergistic benefits and enhanced inactivation efficiency for enteric microorganisms compared to individual PAA, UV, H_2O_2 and UV/H_2O_2 treatments.[17,20,21] If UV and PAA were applied sequentially, then introducing PAA before UV irradiation was more efficient for disinfection than the opposite order.[9,21] The synergistic effect of UV/PAA for disinfection may be attributed to the formation of hydroxyl radical (•OH) and "active" oxygen from the photolysis of

Received: September 12, 2017
Revised: November 16, 2017
Accepted: November 17, 2017
Published: November 17, 2017

DOI: 10.1021/acs.est.7b04694
Environ. Sci. Technol. 2017, 51, 14217−14224

PAA.[9,21] Thus, the application of combined UV and PAA for wastewater disinfection may considerably reduce the disinfectant dosage, contact time, and costs.[17,22]

PAA can be activated by UV light or certain catalysts to generate radicals; thus, the UV/PAA process can be classified as an advanced oxidation process (AOP).[9,17,21−24] Under UV irradiation, homolytic cleavage of PAA's O−O bond occurs to generate acetyloxyl radical ($CH_3C(=O)O^{\bullet}$) and $^{\bullet}OH$ (eq 1).[9,21] Subsequently, $CH_3C(=O)O^{\bullet}$ rapidly dissociates to methyl radical ($^{\bullet}CH_3$) and CO_2, and $^{\bullet}CH_3$ may combine with oxygen to produce a weak peroxy radical ($CH_3O_2^{\bullet}$) (eqs 2 and 3).[9] Meanwhile, $^{\bullet}OH$ may attack the PAA molecule (eqs 4−6).[9] $CH_3C(=O)O^{\bullet}$ may also react with PAA to produce acetylperoxyl radical ($CH_3C(=O)O_2^{\bullet}$) (eq 7).[24] The various radicals formed in the UV/PAA process may exhibit different reactivities. Furthermore, because some amounts of H_2O_2 are always present in PAA solutions, the UV/H_2O_2 AOP coexists in the UV/PAA process.

$$CH_3C(=O)O_2H \xrightarrow{h\nu} CH_3C(=O)O^{\bullet} + {}^{\bullet}OH \quad (1)$$

$$CH_3C(=O)O^{\bullet} \rightarrow {}^{\bullet}CH_3 + CO_2 \quad (2)$$

$$^{\bullet}CH_3 + O_2 \rightarrow CH_3OO^{\bullet} \quad (3)$$

$$CH_3C(=O)O_2H + {}^{\bullet}OH \rightarrow CH_3C(=O)O_2^{\bullet} + H_2O \quad (4)$$

$$CH_3C(=O)O_2H + {}^{\bullet}OH \rightarrow CH_3C(=O)^{\bullet} + O_2 + H_2O \quad (5)$$

$$CH_3C(=O)O_2H + {}^{\bullet}OH \rightarrow CH_3C(=O)OH + {}^{\bullet}OOH \quad (6)$$

$$CH_3C(=O)O_2H + CH_3C(=O)O^{\bullet} \rightarrow CH_3C(=O)O_2^{\bullet} + CH_3C(=O)OH \quad (7)$$

It is well-known that $^{\bullet}OH$ can react rapidly with many micropollutants ($k = 10^6$−10^{10} $M^{-1}\cdot s^{-1}$).[25] Mukhopadhyay et al. reported that UV/PAA could achieve >95% mineralization of 4-chlorophenol.[26] The formation of $^{\bullet}OH$ and other radicals from UV/PAA will be beneficial for elimination of emerging contaminants but has been scarcely investigated. In this study, seven target pharmaceuticals, bezafibrate (BZF), carbamazepine (CBZ), clofibric acid (CA), diclofenac (DCF), ibuprofen (IBP), ketoprofen (KEP), and naproxen (NAP) (structures in Supporting Information (SI) Figure S1), were selected because of their frequency of occurrence in aquatic environments and representation of a wide range of compound structures. The objective was to elucidate the reaction mechanisms and assess the roles of radical species of UV/PAA in degrading the pharmaceuticals. As a necessary step, the photolysis of PAA under UV irradiation was also studied by measuring PAA's light absorption, quantum yields, and scavenging effects on $^{\bullet}OH$. The reactive species responsible for pharmaceutical degradation under UV/PAA were systematically evaluated by a combination of experiments and kinetic simulations. The degradation products of pharmaceuticals by UV/PAA were also evaluated and compared to those by UV/H_2O_2. To the best of our knowledge, this study is among the first to reveal the degradation kinetics and mechanism of pharmaceuticals by UV/PAA, and to systematically investigate the photolysis behavior of PAA.

MATERIALS AND METHODS

Chemicals. Sources of chemicals and reagents are provided in the SI Text S1.

Determination of PAA. The PAA stock solution (39% PAA and 6% H_2O_2, stored at 5 °C) was regularly calibrated by using iodometric titration methods. PAA working solution (10 g/L) was prepared weekly by diluting the standardized PAA stock solution and stored at 5 °C. Residual PAA in experiments was quantified by the *N*,*N*′-diethyl-*p*-phenylenediamine (DPD) colorimetric method. The titration methods are described in SI Text S2.

UV Instrument. The irradiation experiments were conducted in a magnetically stirred 100 mL cylindrical quartz reactor similar to that previously described.[27,28] UV irradiation was supplied from one side of the reactor by a 4-W low pressure UV lamp (G4T5 Hg lamp, Philips TUV4W) peaking at 254 nm in a photochamber at ambient temperature (25 °C) (SI Figure S2). The lamp was warmed up for at least 30 min before the experiments. The effective light path length (L) was measured to be 3.545 cm according to an approach previously described.[27,28] The incident light intensity (I_0) for the quartz reactor was measured to be 2.12×10^{-6} Einstein/(L·s), through the potassium ferrioxalate actinometry method[29] and conversion of the area-metric light intensity (W/cm^2) into that in volumetric unit (Einstein/(L·s)).[27]

Photolysis of PAA. The PAA^0 solution (1 g/L) at pH about 3.17 was prepared by diluting the PAA working solution with deionized water and PAA^0 accounted for >99% of total PAA. The PAA^- solution (1 g/L) was prepared by diluting the PAA stock solution with borate buffer to achieve pH 9.93 at which PAA^- accounted for >98% of total PAA. The total absorbance of PAA^0 or PAA^- solutions containing H_2O_2 was measured with an Agilent UV−vis spectrophotometer, and the absorbance of PAA^0 or PAA^- was obtained by subtracting the H_2O_2 absorbance from the total absorbance. The molar absorption coefficients of H_2O_2, PAA^0 and PAA^- at 200−400 nm were obtained by dividing absorbance by the molar concentration according to the Beer−Lambert Law. Direct photolysis of PAA^0 and PAA^- by UV was conducted at pH 5.09 and 9.65 with or without the existence of the $^{\bullet}OH$ scavenger *tert*-butyl alcohol (TBA) (10 mM). A 2 mL aliquot was sampled from the reactor periodically to measure the residual PAA.

Degradation Experiments. The reaction solution including the individual pharmaceutical was prepared into the quartz reactor with the phosphate or borate buffer (10 mM). Then, the reactor was placed into the photochamber with a running magnetic stirrer. Immediately, a certain volume of PAA working solution was added into the reactor to initiate the reaction. Sample aliquots (1 mL) were drawn from the reactor periodically and promptly put into amber glass vials containing excess sodium thiosulfate ($[Na_2S_2O_3]/[PAA]_0 > 5$) to quench oxidants. Control experiments under UV alone or UV/H_2O_2 were also conducted. Quenching experiments were conducted by adding 10 mM TBA into reaction solutions before UV irradiation. Experiments without UV irradiation were conducted to evaluate pharmaceutical degradation by PAA alone. All experiments were conducted in duplicate or triplicate and the average results are presented.

Analytical Methods. The analytical methods to measure the target pharmaceuticals, model compounds and transformation products are detailed in SI Text S3.

DOI: 10.1021/acs.est.7b04694
Environ. Sci. Technol. 2017, 51, 14217−14224

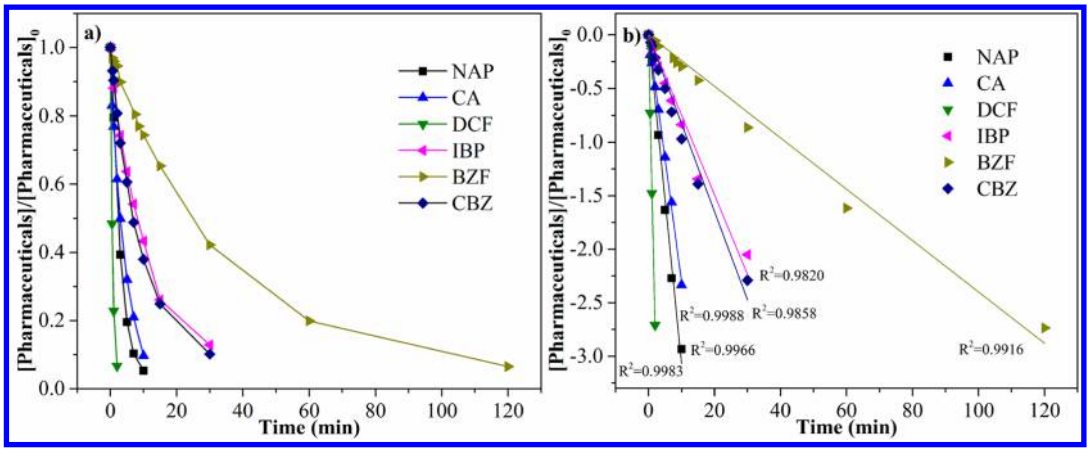

Figure 1. (a) Degradation of pharmaceuticals under the UV/PAA (1 mg/L) process at pH 7.10; (b) ln([pharmaceutical]/[pharmaceutical]$_0$) versus time. Initial pharmaceutical concentration was 1 μM.

Table 1. Pseudo-First-Order Rate Constants (k_{obs}, min^{-1}) of Pharmaceuticals under UV/PAA, UV/H_2O_2, and UV alone[a]

compounds	$k_{UV/PAA}$	k_{UV/H_2O_2}	k_{UV}	$k_{UV/PAA}/k_{UV/H_2O_2}$
bezafibrate (BZF)	(2.40 ± 0.06)×10^{-2}	(2.14 ± 0.01)×10^{-2}	(2.01 ± 0.04)×10^{-2}	1.1
diclofenac (DCF)	1.38 ± 0.03	1.31 ± 0.03	1.09 ± 0.01	1.1
clofibric acid (CA)	(2.30 ± 0.03)×10^{-1}	(1.77 ± 0.05)×10^{-1}	(1.95 ± 0.04)×10^{-1}	1.3
ibuprofen (IBP)	(8.83 ± 0.15)×10^{-2}	(6.41 ± 0.17)×10^{-2}	(2.61 ± 0.07)×10^{-2}	1.4
naproxen (NAP)	(3.07 ± 0.07)×10^{-1}	(8.07 ± 0.42)×10^{-2}	(5.10 ± 0.31)×10^{-2}	3.8
carbamazepine (CBZ)	(8.25 ± 0.31)×10^{-2}	(2.11 ± 0.05)×10^{-2}	(4.9 ± 0.25)×10^{-3}	3.9

[a]Experimental conditions: [pharmaceutical]$_0$ = 1 μM, [PAA]$_0$ = 1 mg/L, [H_2O_2]$_0$ = 0.11 mg/L in UV/H_2O_2 experiments, [phosphate buffer] = 10 mM, pH 7.10, 25 ± 1 °C.

RESULTS AND DISCUSSION

Photolysis of PAA under UV Irradiation. To fully understand the degradation mechanism of pharmaceuticals by UV/PAA, the photolysis of PAA under UV irradiation needs to be understood first. The molar absorption coefficients (ε) of PAA^0, PAA^-, and H_2O_2 at 200−400 nm were determined (SI Figure S3a). The measured ε_{H2O2} at 254 nm was 18.54 $M^{-1}cm^{-1}$, similar to the literature value (18.7 $M^{-1}cm^{-1}$).[30] The ε_{PAA0} and ε_{PAA^-} at 254 nm were 10.01 $M^{-1}cm^{-1}$ and 58.89 $M^{-1}cm^{-1}$, respectively. PAA^- showed much higher UV absorption, about 6 times of PAA^0 and 3 times of H_2O_2.

The photolysis of PAA^0 (pH 5.09) and PAA^- (pH 9.65) under UV irradiation followed first-order kinetics (SI Figure 3b,c). PAA^- has a faster photolysis rate than PAA^0, in accordance with its higher UV absorption at 254 nm. Adding TBA partially inhibited the photolysis of both PAA^0 and PAA^- (more pronounced in the case of PAA^0), confirming that $^{\bullet}OH$ was generated in PAA photolysis and $^{\bullet}OH$ could further react with PAA. Note that scavengers specific for the other radicals possibly formed from PAA photolysis (eqs 1−7) have not been established and information regarding the reactivity of PAA to radical species is scarce in the literature. Nevertheless, we hypothesized that the decay of PAA in UV photolysis was due mainly to direct photolysis and partly to indirect photolysis with $^{\bullet}OH$, on the basis that eq 1 is the dominant reaction for PAA photolysis, and the other radicals likely have lower reactivity than $^{\bullet}OH$. Thus, the rate constants of PAA photolysis obtained under UV+TBA were employed as the direct photolysis rate constants to calculate the quantum yields ($\Phi_{254\ nm}$) of PAA^0 and PAA^-, which were 1.20 mol·Einstein^{-1} and 2.09 mol·Einstein^{-1}, respectively (SI Text S4). They are considerably higher than the reported $\Phi_{254\ nm}$ (0.5 mol·Einstein^{-1})[31] of H_2O_2, indicating that the photolysis of PAA may generate more $^{\bullet}OH$ and/or other active radicals compared to the photolysis H_2O_2 to initiate the radicals' chain reactions.

Assuming that the indirect photolysis of PAA is primarily attributed to $^{\bullet}OH$, the scavenging effects of PAA^0 and PAA^- on $^{\bullet}OH$ was evaluated by measuring the second-order rate constants of PAA^0 or PAA^- with $^{\bullet}OH$ at pH 6.07 and 9.65, respectively, using competition kinetics with *para*-chlorbenzoic acid (*p*CBA) as the chemical probe in a UV/H_2O_2 system (detailed in SI Text S5). The obtained rate constants were $k_{^{\bullet}OH/PAA^0}$ = (9.33 ± 0.3) × 10^8 $M^{-1}\cdot s^{-1}$ and $k_{^{\bullet}OH/PAA^-}$ = (9.97 ± 2.3) × 10^9 $M^{-1}\cdot s^{-1}$. To the best of our knowledge, this is the first report of the $^{\bullet}OH$ rate constants for PAA^0 and PAA^-. These rate constants are 1−2 orders of magnitude higher than that of H_2O_2 ($k_{^{\bullet}OH/H_2O_2}$ = 2.7 × 10^7 $M^{-1}\cdot s^{-1}$),[32] indicating that PAA has a strong scavenging effect on $^{\bullet}OH$ under high PAA concentration or alkaline pH (PAA^- dominance) conditions.

Removal Efficacy of Pharmaceuticals by PAA and UV/PAA. Little degradation of the seven pharmaceuticals occurred with 1 mg/L (i.e., 13.1 μM) PAA at pH 7.10 after 1 h (SI Figure S4a). After increasing PAA dose to 1 g/L (including 0.11 g/L H_2O_2) and reaction time to 24 h, only NAP and DCF showed notable elimination (62.50% and 29.70%, respectively) but the removal for most pharmaceuticals was still less than 11% (SI Figure S4b). Thus, PAA has low reactivity toward the investigated pharmaceuticals and is not an effective oxidant to eliminate such structures.

In contrast, the pharmaceuticals were degraded by more than 93.5% under UV/PAA ([PAA]$_0$ = 1 mg/L) after 2 h of reaction at pH 7.10 (Figure 1a). The degradation of pharmaceuticals by UV/PAA followed pseudo-first-order kinetics (Figure 1b). Because UV alone without PAA was able to rapidly degrade

DOI: 10.1021/acs.est.7b04694
Environ. Sci. Technol. 2017, 51, 14217−14224

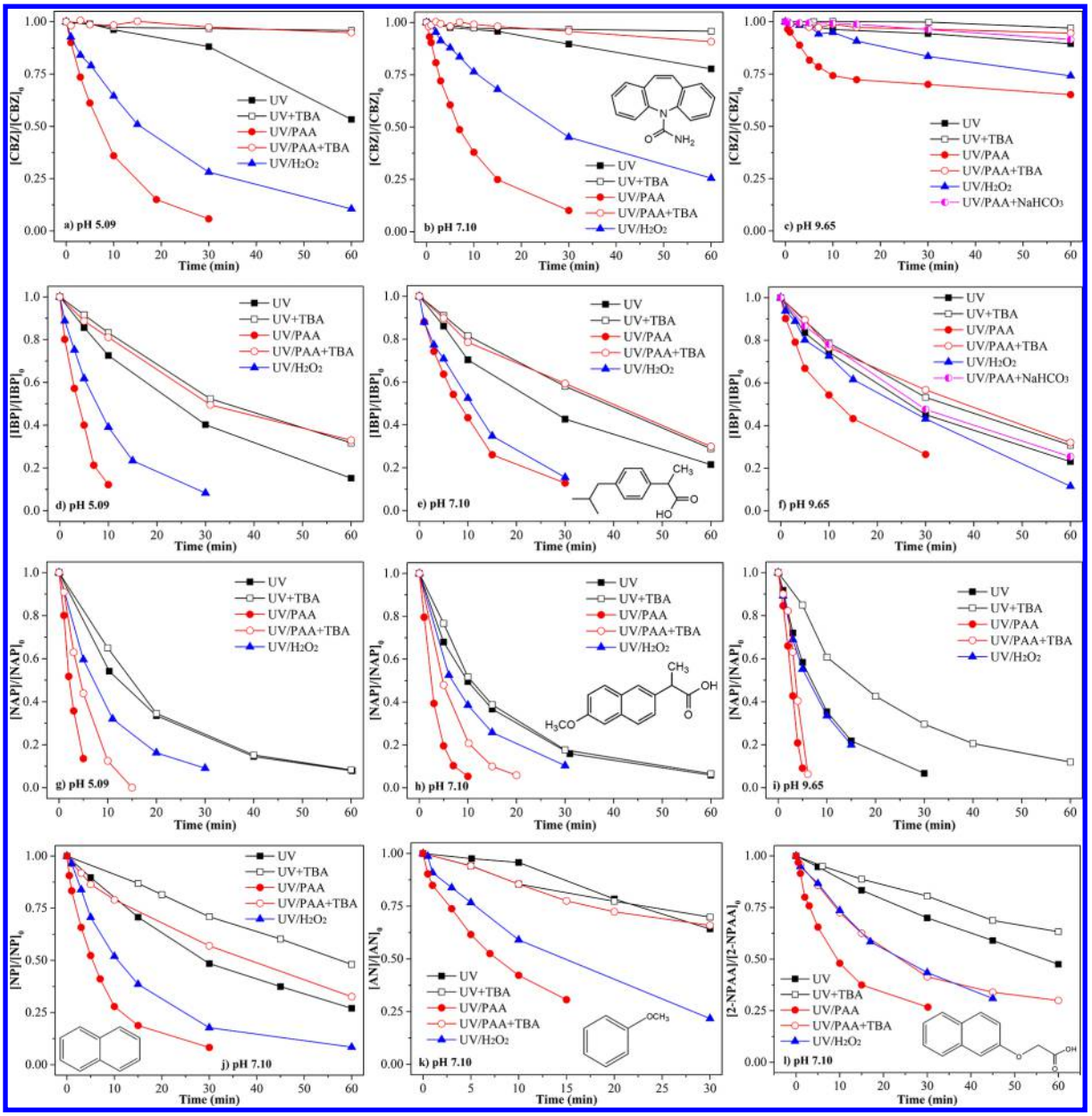

Figure 2. Degradation of pharmaceuticals (CBZ, IBP, and NAP) and substructure compounds (NP, AS, and 2-NPAA) under different conditions. Experimental conditions: $[\text{target compound}]_0$ = 1 μM, $[\text{PAA}]_0$ = 1 mg/L, $[H_2O_2]_0$ = 0.11 ± 0.01 mg/L, $[\text{TBA}]_0$ = 10 mM, $[NaHCO_3]_0$ = 25.9 mM, [buffer] = 10 mM, 25 °C.

KEP (<0.05 μM remained after 2 min), consistent with the literature,[33] KEP was not investigated for UV/PAA.

Table 1 summarizes the obtained rate constants (k_{obs} in min^{-1}) for six pharmaceuticals under UV/PAA, UV/H_2O_2, and UV alone, respectively. The UV/H_2O_2 experiments employed 0.11 mg/L (i.e., 3.3 μM) initial H_2O_2 concentration similar to that in the PAA reaction solution, and represented the UV/H_2O_2 reactions coexistent in the UV/PAA process. The values of k_{UV} for BZF, CA, and DCF were close to $k_{UV/PAA}$, indicating that direct photolysis played a major role in their degradation under UV/PAA. For IBP, NAP, and CBZ, UV/PAA promoted degradation by 3−16 folds compared with UV alone. The influence of UV/H_2O_2 on pharmaceuticals' degradation in the UV/PAA process could be assessed by calculating the $k_{UV/PAA}/k_{UV/H_2O_2}$ ratio (Table 1). For IBP, NAP, and CBZ, the $k_{UV/PAA}/k_{UV/H_2O_2}$ ratios were greater than 1.3, indicating that UV/PAA played a greater role than UV/H_2O_2 in their degradation in the UV/PAA process. Furthermore, the much faster degradation of NAP and CBZ by UV/PAA than by UV/H_2O_2 suggested that some reactive species formed from photolysis of PAA probably contributed to compound degradation.

CBZ, IBP, and NAP Degradation by UV/PAA. As Table 1 shows, CBZ, IBP, and NAP deserve further investigation for their degradation mechanisms under UV/PAA. Thus, the effects of TBA (presence or absence) and pH (5.09, 7.10 and 9.65) on the degradation of CBZ, IBP, and NAP under UV, UV/PAA, and UV/H_2O_2 were examined and shown in Figure 2.

Effect of TBA. For *CBZ* (Figure 2a−c), the comparison between UV alone and UV+TBA suggested that direct photolysis was insignificant over 2 h of irradiation and the modest degradation of CBZ under UV irradiation was primarily

DOI: 10.1021/acs.est.7b04694
Environ. Sci. Technol. 2017, 51, 14217−14224

attributed to •OH. Comparison between UV/PAA and UV/PAA+TBA showed that CBZ degradation under UV/PAA was almost completely inhibited when TBA was added, suggesting that •OH produced from the UV/PAA process was the dominant radical to degrade CBZ. For *IBP* (Figure 2d–f), both direct photolysis and •OH contributed to the degradation of IBP under UV irradiation and the direct photolysis was more important than •OH. After adding TBA, the resultant IBP degradation under UV/PAA was similar to that under UV+TBA. This result means that TBA entirely suppressed the indirect photolysis of IBP under UV/PAA and UV conditions, indicating that •OH oxidation and direct photolysis were likely the main mechanisms of IBP degradation in the UV/PAA process. For *NAP* (Figure 2g–i), direct photolysis mainly contributed to NAP degradation under UV irradiation at acidic and neutral pH, whereas both direct photolysis and •OH contributed to NAP degradation under UV at alkaline pH. Notably, comparison between UV/PAA and UV/PAA+TBA showed a different behavior for NAP. TBA addition only slightly inhibited NAP degradation by UV/PAA especially at alkaline pH, indicating that •OH was not the main radical but other radicals generated from UV/PAA contributed to NAP degradation.

The UV/H_2O_2 results are also shown in Figure 2 and represented the pharmaceutical degradation by background UV/H_2O_2 with the amount of H_2O_2 present in the PAA reaction solution. For all three pharmaceuticals and at the different pHs, UV/PAA contributed more to the pharmaceutical degradation than UV/H_2O_2, consistent with results in Table 1.

Effect of pH. The degradation of CBZ, IBP, and NAP under UV/PAA, UV/PAA+TBA, UV/H_2O_2, UV, and UV+TBA generally showed similar trends across the pH from 5.09 to 9.65 (Figure 2). The degradation rates under UV/PAA at pH 5.09 were slightly faster than or comparable to those at pH 7.10 for all three pharmaceuticals. In contrast, the degradation rates under UV/PAA at pH 9.65 were slower than those at pH 7.10 for CBZ and IBP. The slower UV/PAA reaction rate at alkaline pH could be explained by the stronger •OH scavenging effect and higher photolysis rate of PAA^- than PAA^0. Under UV irradiation at alkaline pH, PAA concentration declined over time and was depleted after 15 min of irradiation (>90% consumption, SI Figure S3c). During this process, the formed radicals reacted with pharmaceuticals and at the same time the generated •OH was scavenged by PAA until the depletion of PAA. After that, residual CBZ and IBP were degraded by UV alone due to the absence of radicals. This phenomenon was well demonstrated in CBZ degradation, which approached a plateau after 15 min due to its very slow direct photolysis (Figure 2c). Additionally, as •OH scavengers, dissolved carbonate/bicarbonate ($k_{\bullet OH/CO_3^{2-}}$ = 3.9 × 10^8 $M^{-1}\cdot s^{-1}$; $k_{\bullet OH/HCO_3^-}$ = 8.5 × 10^6 $M^{-1}\cdot s^{-1}$)[32] are present at higher concentrations in alkaline pH solutions from dissolution of CO_2 from air. Supplemental experiments at pH 9.56 with the addition of $NaHCO_3$ (25.9 mM) were conducted to investigate the effect of carbonate/bicarbonate on the degradation of CBZ and IBP by UV/PAA (Figure 2c,f). As expected, after adding $NaHCO_3$, the degradation of CBZ by UV/PAA for 1 h decreased from 35% to 8.5%. Similarly, the rate constant of IBP degradation by UV/PAA decreased from 0.060 min^{-1} to 0.023 min^{-1}, close to the direct photolysis rate constant. The above results indicate that dissolved CO_2 in the solution can interfere with the degradation of CBZ and IBP by UV/PAA.

In contrast, NAP showed a slightly faster degradation rate by UV/PAA at pH 9.65 than at pH 7.10 (Figure 2i). Because the reaction of NAP with other radicals produced in the UV/PAA process played a more important role in NAP degradation, the greater scavenging effects on •OH at higher pH had less impact on the degradation rate of NAP.

Roles of Radicals in Pharmaceutical Degradation by UV/PAA. *Contributions of UV, •OH, and other Radicals.* The UV/PAA process degrades pharmaceuticals by a combination of direct photolysis, oxidation by •OH and oxidation by other radicals. The contribution of each process was estimated based on the rate constants (min^{-1}) obtained under UV+TBA, UV/PAA, and UV/PAA+TBA according to eqs 8–11.

$$k_{UV/PAA}(min^{-1}) = k_{direct\ photolysis} + k_{\bullet OH\ oxidation} + k_{other\ radicals\ oxidation} \quad (8)$$

$$k_{direct\ photolysis} = k_{UV+TBA} \quad (9)$$

$$k_{other\ radicals\ oxidation} = k_{UV/PAA+TBA} - k_{UV+TBA} \quad (10)$$

$$k_{\bullet OH\ oxidation} = k_{UV/PAA} - k_{UV/PAA+TBA} \quad (11)$$

As Figure 3 shows, direct photolysis had small (IBP and NAP) or little (CBZ) contribution to the degradation under

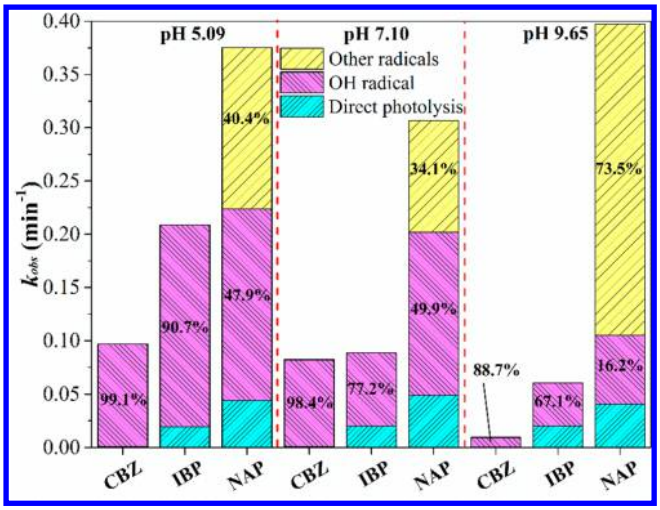

Figure 3. Contributions of direct photolysis, •OH and other radicals to CBZ, IBP, and NAP degradation under UV/PAA at different pH.

UV/PAA. The •OH radical played the major role (77–99% contribution) in the degradation of CBZ and IBP by UV/PAA, and also contributed (16–50%) to the degradation of NAP by UV/PAA. The other radicals produced in the UV/PAA process played an important role in NAP degradation, contributing to 34–40% at acidic and neutral pH, and 74% at alkaline pH. Most of the other radicals are carbon-centered radicals (eqs 1–5, and 7). Evidently, they exhibited structural selectivity in reacting rapidly with NAP but not CBZ and IBP.

Reactive Groups on NAP. To probe the reactivity of NAP to the other radicals, substructures related to NAP, including naphthalene (NP), anisole (AS), and 2-naphthoxyacetic acid (2-NPAA), were selected to examine their degradation under UV/PAA at pH 7.10 using a similar experimental approach. As Figure 2j–l shows, the addition of TBA almost completely inhibited the indirect photolysis of NP and AS, indicating that

DOI: 10.1021/acs.est.7b04694
Environ. Sci. Technol. 2017, 51, 14217–14224

the naphthalene ring without substituents and methoxybenzene are unreactive to the carbon-centered radicals. Interestingly, the degradation of 2-NPAA by UV/PAA was only partly suppressed by TBA, which was similar to NAP. Both 2-NPAA and NAP are naphthyl compounds, suggesting that the presence of substituents on a naphthalene ring may render it more easily attacked by carbon-centered radicals. Note that the propanoic acid group of NAP is unlikely a reactive site to the other radicals, since this functional group is also present in IBP and IBP is not reactive to the other radicals.

The contributions of direct photolysis, $^{\bullet}OH$ and other radicals to the degradation of NP, AS, and 2-NPAA under UV/PAA at pH 7.10 were also estimated and the results are shown in SI Table S1. For NP and AS, their degradation under UV/PAA was mainly attributed to $^{\bullet}OH$ (>82% contribution), and the effect of other radicals was minimum (only 3−6%). In contrast, the other radicals contributed 31.5% to the degradation of 2-NPAA under UV/PAA, which was similar to the 34.1% contribution in the case of NAP. A similar degradation pattern was observed by Zhou et al., who applied an activated carbon fibers (ACFs)/PAA catalytic system to remove organic dyes containing the naphthyl group.[23] By radical scavenging experiments, they also found that TBA only slightly inhibited the removal of RR X-3B and $^{\bullet}OH$ was not the sole active species in the ACFs/PAA system.

Kinetic Modeling for $^{\bullet}OH$ Reactions. To further assess the roles of radicals in the degradation of CBZ, IBP, and NAP under UV/PAA, a kinetic model was established assuming that the degradation of pharmaceuticals under UV/PAA depended on direct photolysis and $^{\bullet}OH$. A simplified pseudosteady-state method widely used for UV/H_2O_2 was modified for the UV/PAA experimental conditions to estimate the steady-state concentration of $^{\bullet}OH$ ($[^{\bullet}OH]_{ss}$). The kinetic modeling employs the $\Phi_{254\ nm}$ and $k_{^{\bullet}OH}$ of PAA^0 and PAA^- determined in this study and is detailed in SI Text S6 and Table S2. Reactions involving the other radicals could not be included in the kinetic model due to the lack of reported rate constants.

The modeling was conducted for UV/PAA and UV/H_2O_2, respectively, and results are presented in SI Figure S5. The model agreed well with the experimental data for degradation of CBZ, IBP, and NAP under UV/H_2O_2. For UV/PAA, the model predicted the degradation of CBZ and IBP reasonably well at acidic and neutral pH, but considerably underestimated their degradation at alkaline pH. One reason for this underestimation was probably due to different HCO_3^-/CO_3^{2-} concentrations in the model and the actual reaction solutions. The model assumed saturated dissolved CO_2 in the solution, while the experiments were conducted with or without addition of 25.9 mM $NaHCO_3$. As shown for IBP degradation, the model agreed much better with the experimental data obtained in solutions spiked with $NaHCO_3$ than those without. As expected, the model significantly underestimated the degradation of NAP under UV/PAA at all pHs due to overlooking the contribution of other radicals, and further confirmed their involvement in NAP degradation under UV/PAA.

Generation and Reactivity of Radicals from UV/PAA. To date, few studies actually investigated the generation of radicals under UV/PAA. The homolysis of PAA to form $^{\bullet}OH$ and other carbon-centered radicals was observed in other activated PAA processes by certain catalysts (e.g., MnO_2 and activated carbon fibers).[23,24] By total energy analysis of the reaction pathway, Rokhina et al. inferred that eq 1 was the rate-determining step in the catalytic PAA oxidation system and that eqs 2−7 were nearly spontaneous.[24] Shi et al. also proposed that the eq 1 was the rate-determining step in the reaction of secondary amines with peracids.[34] Due to the low activation barrier for hydrogen abstraction of PAA, once the primary radicals ($CH_3C(=O)O^{\bullet}$ and $^{\bullet}OH$) formed, it was easy to generate $CH_3C(=O)O_2^{\bullet}$ (eqs 4 and 7).[34] Moreover, $CH_3C(=O)O_2^{\bullet}$ was among the most powerful oxidizing peroxyl radicals, which can rapidly react with TMPD, ABTS, ascorbate, and $O_2^{\bullet-}$ during a pulse radiolysis process at close to diffusion-controlled rates (k = 10^8−10^9 $M^{-1}\cdot s^{-1}$).[35]

Alternatively, the decarboxylation of $CH_3C(=O)O^{\bullet}$ (eq 2) is the most typical β-cleavage reaction,[36] which is irreversible due to formation of stable CO_2 gas, with estimated rate constants of 10^9−10^{10} s^{-1} (65 °C)[37] or 1.6×10^9 s^{-1} (60 °C).[38] However, $^{\bullet}CH_3$ is usually limitedly available in oxygen saturated environments because it can rapidly react with O_2 (4.1×10^9 $M^{-1}\cdot s^{-1}$) to form $CH_3O_2^{\bullet}$.[39] Compared with $CH_3C(=O)O_2^{\bullet}$, $CH_3O_2^{\bullet}$ is a weak peroxy radical, with rate constants ranging from ~10^5 to 10^7 $M^{-1}\cdot s^{-1}$ with various compounds.[40,41] Thus, the relevant radicals in UV/PAA+TBA may include $CH_3C(=O)O^{\bullet}$, $CH_3C(=O)O_2^{\bullet}$, $^{\bullet}CH_3$, and $CH_3O_2^{\bullet}$. Additional NAP degradation experiments were performed under UV/PAA+TBA with N_2 purging for >30 min prior to experiments, to assess the importance of $^{\bullet}CH_3$ and $CH_3O_2^{\bullet}$. The dissolved oxygen in solutions with and without N_2 purging was 0.35 and 4.96 mg/L, respectively. N_2 purging only slightly decreased NAP removal from 82.69% to 77.38% after 7 min reaction at pH 7.10 (data not shown), implying that $^{\bullet}CH_3$ and $CH_3O_2^{\bullet}$ were not critical species. Consequently, $CH_3C(=O)O^{\bullet}$ as a primary radical and $CH_3C(=O)O_2^{\bullet}$ as a highly reactive radical were more likely to selectively degrade NAP under UV/PAA. More research is needed for direct detection of these radicals and assessing their reactivity.

Products Evaluation. The transformation products of pharmaceuticals by UV/PAA were evaluated and compared to those by UV/H_2O_2. Modified experimental conditions were employed to generate higher concentrations of products. The products' MS information, evolution, and proposed structures are detailed in SI Text S7, Tables S3−S5, Figures S6−S10, and Figure 4. Overall, degradation of CBZ, IBP, and NAP by UV/PAA or UV/H_2O_2 generated many products. A greater number of different products was found under UV/PAA than UV/H_2O_2, although many products were similar in both AOPs (SI Tables S3−S5). Hydroxylation and/or oxygenation products were found in all cases (including m/z of 226, 242, 253a−c, 269a−d, 271a−c, 283, and 287 for CBZ (SI Figure S7); m/z of 193a,b and 223a,b for IBP (SI Figure S9); m/z of 189, 203a,b, 233a,b, and 247a−d for NAP (Figure 4)), indicating the involvement of $^{\bullet}OH$. IBP also underwent decarboxylation (i.e., m/z 161 and 177a,b (SI Figure S9)), whereas NAP could lose a methyl group, the methoxy group or water (i.e., m/z 129, 143, 201, 203, and 231b (Figure 4)). The similar products in UV/PAA and UV/H_2O_2 for CBZ and IBP were consistent with the finding that $^{\bullet}OH$ played the major role in their degradation by both AOPs. Degradation of NAP by UV/PAA generated the highest number of different products. However, products that are linked to attack of $CH_3CO_2^{\bullet}$ or $CH_3CO_3^{\bullet}$ were not found. This might be due to the experimental conditions used for product generation and low abundance or transient nature of these products.

Environmental Significance. PAA is an alternative disinfectant with growing usage, and this study is among the

DOI: 10.1021/acs.est.7b04694
Environ. Sci. Technol. 2017, 51, 14217−14224

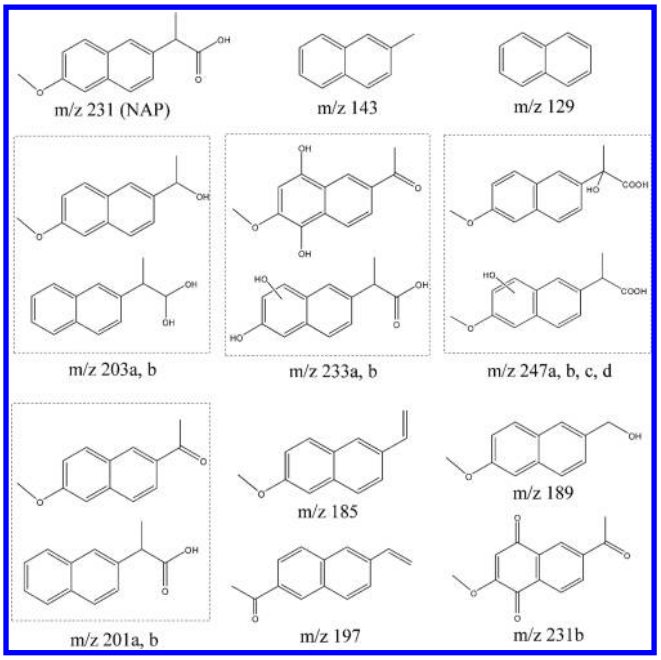

Figure 4. Structures of NAP and proposed transformation products.

first to demonstrate that UV/PAA can be an effective AOP for pharmaceuticals elimination. The photolysis of PAA under UV irradiation was characterized to improve the understanding of reaction kinetics under UV/PAA. Notably, this study identified the importance of new critical reactive species (i.e., carbon-centered radicals $CH_3C(=O)O^{\bullet}$ and $CH_3C(=O)O_2^{\bullet}$), apart from $^{\bullet}OH$, to contribute to the degradation of naphthyl-containing compounds (NAP and 2-NAPP) by UV/PAA. The new knowledge obtained by this study offers an important basis for further research on UV/PAA and other photoactivated PAA processes. The UV activation of PAA appears to be advantageous over that of H_2O_2 for the higher quantum yield and additional reactivity of carbon-centered radicals for certain compounds' degradation. However, PAA poses a stronger scavenging effect on $^{\bullet}OH$ than H_2O_2. More research should be conducted to evaluate the efficacy of UV/PAA to degrade a wider range of contaminants in real water matrices, further assess the reactivity and structural selectivity of the carbon-centered radicals, and assess the toxicity of the transformation products. Results of this and future work will improve the development of UV/PAA as a new degradation strategy for micropollutants in water and facilitates its optimization.

■ ASSOCIATED CONTENT

Supporting Information

The Supporting Information is available free of charge on the ACS Publications website at DOI: 10.1021/acs.est.7b04694.

Texts S1−S7, Tables S1−S5, and Figures S1−S10 (PDF)

■ AUTHOR INFORMATION

Corresponding Authors

*Phone: 86-010-63226528; fax: 86-010-62336900; e-mail: zhangliqiu@163.com (L.Z.).

*Phone: 404-894-7694; fax: 404-358-7087; e-mail: ching-hua.huang@ce.gatech.edu (C.-H.H.).

ORCID

Ching-Hua Huang: 0000-0002-3786-094X

Notes

The authors declare no competing financial interest.

■ ACKNOWLEDGMENTS

M.C. gratefully acknowledges financial support from the China Scholarship Council. This material is based upon work supported by the National Science Foundation under Grant CHE-1609361. Any opinions, findings, and conclusions or recommendations expressed in this material are those of the authors and do not necessarily reflect the views of the National Science Foundation.

■ REFERENCES

(1) Kitis, M. Disinfection of wastewater with peracetic acid: a review. *Environ. Int.* **2004**, *30* (1), 47−55.

(2) Peroxygen compounds. In *Disinfection, Sterilization, and Preservation*, 5th ed.; Block, S. S., Ed.; Lippincott, Williams, and Wilkins: Philadelphia, 2001; pp 185−205.

(3) Zhao, X.; Zhang, T.; Zhou, Y.; Liu, D. Preparation of peracetic acid from hydrogen peroxide Part I: Kinetics for peracetic acid synthesis and hydrolysis. *J. Mol. Catal. A: Chem.* **2007**, *271*, 246−252.

(4) Luukkonen, T.; Pehkonen, S. Peracids in water treatment: A critical review. *Crit. Rev. Environ. Sci. Technol.* **2017**, *47*, 1−39.

(5) Flores, M. J.; Brandi, R. J.; Cassano, A. E.; Labas, M. D. Kinetic model of water disinfection using peracetic acid including synergistic effects. *Water Sci. Technol.* **2016**, *73* (2), 275−282.

(6) Flores, M. J.; Lescano, M. R.; Brandi, R. J.; Cassano, A. E.; Labas, M. D. A novel approach to explain the inactivation mechanism of Escherichia coli employing a commercially available peracetic acid. *Water Sci. Technol.* **2014**, *69* (2), 358−363.

(7) Yuan, Z.; Ni, Y.; van Heiningen, A. R. P. Kinetics of peracetic acid decomposition. Part I: Spontaneous decomposition at typical pulp bleaching conditions. *Can. J. Chem. Eng.* **1997**, *75*, 37−41.

(8) Alasri, A.; Roques, C.; Michel, G.; Cabassud, C.; Aptel, P. Bactericidal properties of peracctic acid and hydrogen peroxide, alone and in combination, and chlorine, and formaldehyde against bacterial water strains. *Can. J. Microbiol.* **1992**, *38*, 635.

(9) Caretti, C.; Lubello, C. Wastewater disinfection with PAA and UV combined treatment: A pilot plant study. *Water Res.* **2003**, *37* (10), 2365−2371.

(10) Falsanisi, D.; Gehr, R.; Santoro, D.; Dell'Erba, A.; Notarnicola, M.; Liberti, L. Kinetics of PAA demand and its implications on disinfection of wastewaters. *Water Qual. Res. J. Can.* **2006**, *41* (4), 398−409.

(11) Gehr, R.; Wagner, M.; Veerasubramanian, P.; Payment, P. Disinfection efficiency of peracetic acid, UV and ozone after enhanced primary treatment of municipal wastewater. *Water Res.* **2003**, *37* (19), 4573−4586.

(12) Veschetti, E.; Cutilli, D.; Bonadonna, L.; Briancesco, R.; Martini, C.; Cecchini, G.; Anastasi, P.; Ottaviani, M. Pilot-plant comparative study of peracetic acid and sodium hypochlorite wastewater disinfection. *Water Res.* **2003**, *37*, 78−94.

(13) Rossi, S.; Antonelli, M.; Mezzanotte, V.; Nurizzo, C. Peracetic acid disinfection: A feasible alternative to wastewater chlorination. *Water Environ. Res.* **2007**, *79* (4), 341−350.

(14) Pedersen, P. O.; Brodersen, E.; Cecil, D. Disinfection of tertiary wastewater effluent prior to river discharge using peracetic acid; treatment efficiency and results on by-products formed in full scale tests. *Water Sci. Technol.* **2013**, *68* (8), 1852−1856.

(15) US EPA. *Combined Sewer Overflow Technology Fact Sheet: Alternative Disinfection Methods*; EPA832-F-99-033; Washington, DC, Office of Water, 1999.

(16) US EPA. *Alternative Disinfection Methods Fact Sheet: Peracetic Acid*; EPA 832-F-12-030; Washington, DC, Office of Wastewater Management, 2012.

(17) Koivunen, J.; Heinonen-Tanski, H. Inactivation of enteric microorganisms with chemical disinfectants, UV irradiation and

DOI: 10.1021/acs.est.7b04694
Environ. Sci. Technol. 2017, 51, 14217−14224

combined chemical/UV treatments. *Water Res.* **2005**, *39* (8), 1519−1526.
(18) Hey, G.; Ledin, A.; Jansen, J.; Andersen, H. R. Removal of pharmaceuticals in biologically treated wastewater by chlorine dioxide or peracetic acid. *Environ. Technol.* **2012**, *33* (7−9), 1041−1047.
(19) Sharma, S.; Mukhopadhyay, M.; Murthy, Z. V. P. Degradation of 4-chlorophenol in wastewater by organic oxidants. *Ind. Eng. Chem. Res.* **2010**, *49* (7), 3094−3098.
(20) Beber de Souza, J.; Queiroz Valdez, F.; Jeranoski, R. F.; Vidal, C. M. d. S.; Cavallini, G. S. Water and wastewater disinfection with peracetic acid and UV radiation and using advanced oxidative process PAA/UV. *Int. J. Photoenergy* **2015**, *2015*, 1−7.
(21) Lubello, C.; Caretti, C.; Gori, R. Comparison between PAA/UV and H_2O_2/UV disinfection for wastewater reuse. *Water Sci. Technol.* **2002**, *2* (1), 205−212.
(22) Rajala-Mustonen, R. L.; Toivola, P. S.; Heinonen-Tanski, H. Effects of peracetic acid and UV irradiation on the inactivation of coliphages in wastewater. *Water Sci. Technol.* **1997**, *35* (11−12), 237−241.
(23) Zhou, F.; Lu, C.; Yao, Y.; Sun, L.; Gong, F.; Li, D.; Pei, K.; Lu, W.; Chen, W. Activated carbon fibers as an effective metal-free catalyst for peracetic acid activation: Implications for the removal of organic pollutants. *Chem. Eng. J.* **2015**, *281*, 953−960.
(24) Rokhina, E. V.; Makarova, K.; Golovina, E. A.; Van As, H.; Virkutyte, J. Free radical reaction pathway, thermochemistry of peracetic acid homolysis, and its application for phenol degradation: Spectroscopic study and quantum chemistry calculations. *Environ. Sci. Technol.* **2010**, *44* (17), 6815−6821.
(25) Schwarzenbach, R. P.; Gschwend, P. M.; Imboden, D. M. Photochemical transformation reactions. In *Environmental Organic Chemistry*, 3rd ed.; John Wiley and Sons, Inc.: New York, 2016; pp 436−484.
(26) Mukhopadhyay, M.; Daswat, D. P. Photochemical degradation of 4-chlorophenol in the aqueous phase using peroxyacetic acid (PAA). *Water Sci. Technol.* **2012**, *67* (2), 440−445.
(27) Sun, P.; Pavlostathis, S. G.; Huang, C. H. Photodegradation of veterinary ionophore antibiotics under UV and solar irradiation. *Environ. Sci. Technol.* **2014**, *48* (22), 13188−13196.
(28) Zhang, R.; Sun, P.; Boyer, T. H.; Zhao, L.; Huang, C. H. Degradation of pharmaceuticals and metabolite in synthetic human urine by UV, UV/H_2O_2, and UV/PDS. *Environ. Sci. Technol.* **2015**, *49* (5), 3056−3066.
(29) Harris, G.; Adams, V. D.; Moore, W.; Sorensen, D. Potassium ferrioxalate as chemical actinometer in ultraviolet reactors. *J. Environ. Eng.* **1987**, *113* (3), 612−627.
(30) Bolton, J. R.; Cater, S. R. *Homogeneous Photodegradation of Pollutants in Contaminated Water—An Introduction*; Lewis Publishers, Inc.: Boca Raton, 1994; pp 467−490.
(31) Crittenden, J. C.; Hu, S.; Hand, D. W.; Green, S. A. A kinetic model for H_2O_2/UV process in a completely mixed batch reactor. *Water Res.* **1999**, *33* (10), 2315−2328.
(32) Buxton, G. V.; Greenstock, C. L.; Helman, W. P.; Ross, A. B. Critical review of rate constants for reactions of hydrated electrons, hydrogen atoms and hydroxyl radicals (AOH/AO^-) in aqueous solution. *J. Phys. Chem. Ref. Data* **1988**, *17* (2), 513−886.
(33) Pereira, V. J.; Linden, K. G.; Weinberg, H. S. Evaluation of UV irradiation for photolytic and oxidative degradation of pharmaceutical compounds in water. *Water Res.* **2007**, *41* (19), 4413−4423.
(34) Shi, H.-C.; Li, Y. Formation of nitroxide radicals from secondary amines and peracids: A peroxyl radical oxidation pathway derived from electron spin resonance detection and density functional theory calculation. *J. Mol. Catal. A: Chem.* **2007**, *271* (1−2), 32−41.
(35) Schuchmann, M. N.; Von Sonntag, C. The rapid hydration of the acetyl radical. A pulse radiolysis study of acetaldehyde in aqueous solution. *J. Am. Chem. Soc.* **1988**, *110* (17), 5698−5701.
(36) Togo, H. What are free radicals? In *Advanced Free Radical Reactions for Organic Synthesis*; Togo, H., Ed.; Elsevier Inc.: Oxford, 2004; p 8.
(37) Herk, L.; Feld, M.; Szwarc, M. Studies of "cage" reactions. *J. Am. Chem. Soc.* **1961**, *83* (14), 2998−3005.
(38) Braun, W.; Rajbenbach, L.; Eirich, F. R. Peroxide decomposition and cage effect. *J. Phys. Chem.* **1962**, *66* (9), 1591−1595.
(39) Marchaj, A.; Kelley, D. G.; Bakac, A.; Espenson, J. H. Kinetics of the reactions between alkyl radicals and molecular oxygen in aqueous solution. *J. Phys. Chem.* **1991**, *95* (11), 4440−4441.
(40) Huie, R. E.; Neta, P. Rate constants for one-electron oxidation by methylperoxyl radicals in aqueous solutions. Int. *Int. J. Chem. Kinet.* **1986**, *18* (10), 1185−1191.
(41) Neta, P.; Huie, R. E.; Maruthamuthu, P.; Steenken, S. Solvent effects in the reactions of peroxyl radicals with organic reductants. Evidence for proton-transfer-mediated electron transfer. *J. Phys. Chem.* **1989**, *93* (22), 7654−7659.

DOI: 10.1021/acs.est.7b04694
Environ. Sci. Technol. 2017, 51, 14217−14224

Supporting Information

UV/Peracetic Acid for Degradation of Pharmaceuticals and Reactive Species Evaluation

Meiquan Cai[1,2,3], Peizhe Sun[2,4], Liqiu Zhang[1,*], Ching-Hua Huang[*]

[1] *College of Environmental Science and Engineering, Beijing Forestry University, Beijing, 100083, P.R. China.*

[2] *School of Civil and Environmental Engineering, Georgia Institute of Technology, Atlanta, Georgia 30332, United States*

[3] *School of Environment, Tsinghua University, Beijing 100084, P.R. China*

[4] *School of Environmental Science and Engineering, Tianjin University, Tianjin 30072, P.R. China*

[*]Corresponding Authors. Phone: 404-894-7694; Fax: 404-358-7087; E-mail: ching-hua.huang@ce.gatech.edu (Ching-Hua Huang). Phone: 86-010-63226528; Fax: 86-010-62336900; E-mail: zhangliqiu@163.com (Liqiu Zhang)

Texts:	S1-S7
Table:	S1-S5
Figures:	S1-S10
References:	41
Pages:	21

Text S1. Chemicals

Bezafibrate (BZF), carbamazepine (CBZ), clofibric acid (CA), diclofenac (DCF) sodium salt, ibuprofen (IBP), ketoprofen (KEP) and naproxen (NAP) were purchased from Sigma-Aldrich (St. Louis, MO, USA) with the purity >98%. H_2O_2 (30% w/w) solution and *tert*-butyl alcohol (TBA) were obtained from Fisher Scientific (Hampton, NH, USA). PAA (~39 wt% in acetic acid, ≤6% H_2O_2) solution, 2-naphthoxyacetic acid (2-NPAA, 98% purity), naphthalene (NP, 99% purity), *para*-chlorobenzoic acid (*p*CBA, 99% purity), methanol (99.9% purity), sodium hydroxide (NaOH) and sodium thiosulfate ($Na_2S_2O_3$) were obtained from Sigma-Aldrich. Anisole (AS, 99% purity), nitrobenzene (NB, 99.5% purity) and analytical-grade formic acid (99% purity) were purchased from Acros Organics (Geel, Belgium). All other chemicals and reagents used without further purification were analytical grade or above and purchased from Sigma-Aldrich (St. Louis, MO, USA) or Fisher Scientific (Hampton, NH, USA). Reagent water (≥18 mΩ-cm) was produced from a Milli-Q integral water purification system (Millipore, Billerica, MA, USA). BZF, CBZ, CA, IBP, KEP and NAP stock solutions in deionized (DI) water were prepared at 50-200 μM by dissolving the solid of standard compounds according to their water solubility and stored at 5 °C before use. DCF stock solution was prepared in methanol at 5 mM due to its low water solubility and working solution (5 μM) was prepared daily by evaporating methanol from the stock solution and reconstituting in DI water.

Text S2. Determination of PAA

PAA is unstable especially at low concentrations.[1] A solution with 40% of PAA loses about 1-2% of its active ingredient per month.[2] The PAA stock solution (39% PAA and 6% H_2O_2 initially) was stored at 5 °C and regularly calibrated by using titration methods. The sum of PAA and H_2O_2 concentrations was first measured with iodometric titration, by adding potassium iodide (with ammonium molybdate as a catalyst) to produce the liberated iodine and then titrating the iodine with sodium thiosulfate. Then, the concentration of H_2O_2 in PAA solution or in pure H_2O_2 stock solution was titrated with potassium permanganate under acidic pH. The concentration of PAA in the stock solution was calculated by subtracting H_2O_2 concentration from the sum of PAA and H_2O_2 concentrations.

PAA working solution at 10 g/L was prepared weekly by diluting the standardized PAA stock solution and was stored at 5 °C. Residual PAA in experiments was quantified by the *N,N'*-diethyl-*p*-phenylenediamine (DPD) colorimetric method.[3] The sample was treated with an excess amount of potassium iodide. The produced iodine could react with DPD to form a pink-colored species that could be measured by absorbance at 515 nm and was in direct proportion to PAA concentration. Supplementary experiments confirmed that the low concentrations (<2.5 mg/L) of H_2O_2 in the samples had negligible influence on PAA determination by the DPD method.

Text S3. Analytical methods

The loss of target pharmaceuticals, *p*CBA, NB, AS, NP and 2-NPAA was monitored by an Agilent 1100 series high performance liquid chromatography (HPLC) system equipped with a diode-array UV detector (DAD) and an Agilent Zorbax SB-C18 column (2.1 × 150 mm, 5 μm). BZF, CBZ, CA, DCF, IBP, KEP, NAP, *p*CBA, NB, AS, NP, and 2-NPAA were detected at 235, 285, 227, 278, 219, 256, 231, 234, 268, 220, 254 and 226 nm, respectively. Isocratic elution was used with (i) methanol and 0.1% (v/v) formic acid for BZF, CBZ, CA, DCF, IBP, KEP, NAP, *p*CBA and 2-NPAA; (ii) acetonitrile and DI water for NP; and (iii) methanol and DI water for NB and AS. The injection volume was 20 μL except for NAP it was 5 μL.

An Agilent 1100 series HPLC outfitted with an Agilent Zorbax RX-C18 column (2.1 × 150 mm, 5 μm), a DAD, and a single-quadrupole mass spectrometer (MS) was used for the transformation products identification of CBZ, IBP and NAP. HPLC separations were performed with methanol (A) and 0.1% (v/v) formic acid (B) at a flow rate of 0.2 mL/min with gradient elution program. The injection volume was 60 μL. The electrospray ionization at positive mode (ESI+) was applied for CBZ and NAP with the mass scan range of m/z 70-500, whereas both positive (ESI+) and negative (ESI-) modes were applied for IBP. The mass fragmentation voltage was set from 35 to 220 eV. The drying gas flow was 10 L/min. The nebulizer pressure was 45 psig for IBP and NAP, and 40 psig for CBZ. The drying gas temperature was 350 °C for IBP and NAP, and 300 °C for CBZ. The capillary voltage was 4000 V (±).

Text S4. Calculation for the quantum yields (Φ) of PAA^0 and PAA^-

Quantum yields of PAA^0 and PAA^- photolysis at 254 nm were calculated according to Eq. S1:[4]

$$\Phi_{254\,nm} = \frac{k_d \cdot A}{(I_0 \cdot (1-10^{-A \cdot L}) \cdot \varepsilon_{254\,nm})} \quad \text{(S1)}$$

where $\Phi_{254\,nm}$ is the quantum yield at 254 nm (mol/Einstein); k_d is the direct photolysis rate constant experimentally determined under UV+TBA (s^{-1}); $\varepsilon_{254\,nm}$ is the molar absorption coefficient at 254 nm ($M^{-1}\cdot cm^{-1}$); I_0 is the incident light intensity (2.12×10^{-6} Einstein/(L·s)); and L is the effective light path length (3.545 cm). Note that $A = (\varepsilon_{PAA0}[PAA^0]+\varepsilon_{PAA-}[PAA^-]+\varepsilon_{H2O2}[H_2O_2]+\alpha)$, in which α is the absorption coefficient of the solvent (i.e. buffered aqueous solution) (cm^{-1}).

Text S5. Competition kinetics for the second-order rate constants with ·OH

Competition kinetics[4-9] were employed to determine the second-order rate constants of PAA^0, PAA^-, IBP^0 and NAP^0 with ·OH under UV/H_2O_2. The competition kinetic experiments were conducted by spiking H_2O_2 (1 mM) into the reactor containing the competitor (NB (10

μM) or *p*CBA (10 μM or 5 μM)) and the target compound (5 mg/L PAA^0 at pH 6.07, 10 mg/L PAA^- at pH 9.65, or 10 μM individual pharmaceutical at set pH (IBP^0 at pH 2.99; NAP^0 at pH 2.52)) in DI water with phosphate or borate buffer (10 mM), and then the reaction solutions were exposed to UV irradiation. The relatively high H_2O_2 concentration was to ensure the excess H_2O_2 was the main $^{\bullet}OH$ generator and could produce sufficient amounts of $^{\bullet}OH$ by UV photolysis.

As described in literature,[4] the degradation rates of target compound and competitor under UV/H_2O_2 are related to each other according to Eqs. S2 and S3:

$$\ln\left(\frac{\lceil \text{target} \rceil_t}{\lceil \text{target} \rceil_0}\right) - k_{d,\text{target}}t = \left(\ln\left(\frac{\lceil \text{competitor} \rceil_t}{\lceil \text{competitor} \rceil_0}\right) - k_{d,\text{competitor}}t\right)\frac{k_{^{\bullet}OH/\text{target}}}{k_{^{\bullet}OH/\text{competitor}}} \quad \text{(S2)}$$

$$\frac{\left(k_{obs,\text{target}} - k_{d,\text{target}}\right)}{\left(k_{obs,competitor} - k_{d,\text{competitor}}\right)} = \frac{k_{i,\text{target}}}{k_{i,\text{competitor}}} = \frac{k_{^{\bullet}OH/\text{target}}}{k_{^{\bullet}OH/\text{competitor}}} \quad \text{(S3)}$$

where t is time (s), $k_{d,target}$ and $k_{d,competitor}$ are the pseudo-first-order direct photolysis rate constants (in s^{-1}) measured under UV alone; $k_{^{\bullet}OH/target}$ and $k_{^{\bullet}OH/competitor}$ are the second-order rate constants with $^{\bullet}OH$ (in $M^{-1}s^{-1}$); $k_{obs,target}$ and $k_{obs,competitor}$ are the observed pseudo-first-order degradation rate constants (in s^{-1}) under UV/H_2O_2; and $k_{i,target}$ and $k_{i,competitor}$ are the indirect photolysis rate constants (in s^{-1}) which could be obtained by subtracting k_d from k_{obs}.

Before the competition kinetic experiments, control experiments with UV alone and addition of TBA were conducted to obtain the direct photolysis rate constants k_d (i.e., k_{UV+TBA}). Results confirmed that the direct photolysis of NB or *p*CBA by UV alone was negligible. Control experiments were also conducted with NB or *p*CBA in the presence of PAA without UV, and no degradation of NB or *p*CBA was observed (data not shown).

The degradation of NB, *p*CBA, PAA^0, PAA^- and pharmaceuticals followed pseudo-first-order reaction kinetics and thus each k_{obs} was obtained. By applying the known $k_{^{\bullet}OH}$ of NB ($k_{^{\bullet}OH/NB} = 3 \times 10^9\ M^{-1}\cdot s^{-1}$)[10] or *p*CBA ($k_{^{\bullet}OH/pCBA} = 5 \times 10^9\ M^{-1}\cdot s^{-1}$)[11] into Eq. S3, the $k_{^{\bullet}OH}$ values of PAA^0, PAA^- and pharmaceuticals were derived.

Text S6. Predicting the degradation of CBA, IBP and NAP in UV/PAA process.

Estimation for the steady-state concentration of $^{\bullet}OH$ ($[^{\bullet}OH]_{ss}$). In UV/PAA, $^{\bullet}OH$ is mainly generated from the photolysis of PAA^0, PAA^-, H_2O_2 and HO_2^-, which also consumed $^{\bullet}OH$ as radical scavengers. Besides pharmaceuticals, acetic acid and acetate in PAA solution, and carbonate and bicarbonate from dissolved CO_2 also have scavenging effects on $^{\bullet}OH$.[11] Therefore, the formation rate ($F_{^{\bullet}OH}$) and the consumption rate ($C_{^{\bullet}OH}$) of $^{\bullet}OH$ can be express as follows:

$$F_{\bullet OH} = P_{PAA^0} + P_{PAA^-} + P_{H_2O_2} \quad \text{(S4)}$$

$$C_{\bullet OH} = Q_{PAA^0} + Q_{PAA^-} + Q_{H_2O_2} + Q_{HO_2^-} + Q_{HAc} + Q_{Ac^-} + Q_{HCO_3^-} + Q_{CO_3^{2-}} + Q_{compd} \quad \text{(S5)}$$

where P_{PAA0}, P_{PAA-} and P_{H2O2} are the rates of •OH formation from PAA^0, PAA^- and H_2O_2 photolysis; Q_{PAA0}, Q_{PAA-}, Q_{H2O2}, Q_{HO2-}, Q_{HAc}, Q_{Ac-}, Q_{HCO3^-}, $Q_{CO3^{2-}}$ and Q_{compd} are the rates of •OH consumption by PAA^0, PAA^-, H_2O_2, HO_2^-, acetic acid (HAc), acetate (Ac^-), HCO_3^-, CO_3^{2-} and pharmaceutical.

Based on the steady-state assumption, the formation rate of •OH is equal to the consumption rate of •OH, as expressed in Eq. S6, which can be further expressed as Eq. S7 by using the reactions in Table S2.

$$\begin{aligned} F_{\bullet OH} - C_{\bullet OH} &= P_{PAA^0} + P_{PAA^-} + P_{H_2O_2} - (Q_{PAA^0} + Q_{PAA^-} + Q_{H_2O_2} + Q_{HO_2^-} \\ &+ Q_{HAc} + Q_{Ac^-} + Q_{HCO_3^-} + Q_{CO_3^{2-}} + Q_{compd}) = 0 \end{aligned} \quad \text{(S6)}$$

$$\begin{aligned} &\frac{\Phi_{PAA^0} I_0 \varepsilon_{PAA} \left[PAA^0\right]\left(1\text{-}10^{-AL}\right)}{A} + \frac{\Phi_{PAA^-} I_0 \varepsilon_{PAA^-} \left[PAA^-\right]\left(1\text{-}10^{-AL}\right)}{A} + \frac{2\Phi_{H_2O_2} I_0 \varepsilon_{H_2O_2} \left[H_2O_2\right]\left(1\text{-}10^{-AL}\right)}{A} \\ &- k_{PAA^0,\bullet OH}[PAA^0][\bullet OH]_{ss} - k_{PAA^-,\bullet OH}[PAA^-][\bullet OH]_{ss} - k_{H_2O_2,\bullet OH}[H_2O_2][\bullet OH]_{ss} - k_{HO_2^-,\bullet OH}[HO_2^-][\bullet OH]_{ss} \\ &- k_{HAc,\bullet OH}[HAc][\bullet OH]_{ss} - k_{Ac^-,\bullet OH}[Ac^-][\bullet OH]_{ss} - k_{HCO_3^-,\bullet OH}[HCO_3^-][\bullet OH]_{ss} - k_{CO_3^{2-},\bullet OH}[CO_3^{2-}][\bullet OH]_{ss} \\ &- k_{compd,\bullet OH}[Compd][\bullet OH]_{ss} = 0 \end{aligned} \quad \text{(S7)}$$

where Φ_{PAA0}, Φ_{PAA-} and Φ_{H2O2} are the quantum yields of PAA^0, PAA^- and H_2O_2 photolysis at 254 nm; ε_{PAA0}, ε_{PAA-} and ε_{H2O2} are the molar absorption coefficients at 254 nm ($M^{-1}\cdot cm^{-1}$); I_0 is the incident light intensity (2.12×10^{-6} Einstein/(L·s)); L is the effective light path length (3.545 cm); and $A = (\varepsilon_{PAA0}[PAA^0] + \varepsilon_{PAA-}[PAA^-] + \varepsilon_{H2O2}[H_2O_2] + \alpha)$ in which α is the absorption coefficient of the solvent (cm^{-1}). The $[\bullet OH]_{ss}$ can then be expressed as Eq. S8 by solving Eq. S7.

$$\begin{aligned} [\bullet OH]_{ss} = (&\frac{\Phi_{PAA^0} I_0 \varepsilon_{PAA} \left[PAA^0\right]\left(1\text{-}10^{-AL}\right)}{A} + \frac{\Phi_{PAA^-} I_0 \varepsilon_{PAA^-} \left[PAA^-\right]\left(1\text{-}10^{-AL}\right)}{A} \\ &+ \frac{2\Phi_{H_2O_2} I_0 \varepsilon_{H_2O_2} \left[H_2O_2\right]\left(1\text{-}10^{-AL}\right)}{A}) / (k_{PAA^0,\bullet OH}[PAA^0] + k_{PAA^-,\bullet OH}[PAA^-] + k_{H_2O_2,\bullet OH}[H_2O_2] \\ &+ k_{HO_2^-,\bullet OH}[HO_2^-] + k_{HAc,\bullet OH}[HAc] + k_{Ac^-,\bullet OH}[Ac^-] + k_{HCO_3^-,\bullet OH}[HCO_3^-] + k_{CO_3^{2-},\bullet OH}[CO_3^{2-}] + k_{compd,\bullet OH}[Compd]) \end{aligned} \quad \text{(S8)}$$

All components were assumed at constant concentrations during the reaction. The concentrations of HCO_3^- and CO_3^{2-} in carbon dioxide-saturated water were employed for calculation. The $[\bullet OH]_{ss}$ can be calculated by applying the concentrations of each component and their second-order rate constants into Eq. S8.

Modeling the degradation of CBA, IBP and NAP in UV/PAA process. The experimental results indicated that the degradation of CBZ and IBP in UV/PAA was a result of both direct photolysis and •OH oxidation, whereas the NAP degradation was attributed to direct photolysis, •OH and other radicals. The kinetics of CBZ, IBP and NAP degradation in the

UV/PAA process can be modeled as follows:

$$-\frac{\mathrm{d[CBZ]}}{\mathrm{dt}} = k^{s}_{obs,CBZ}[\mathrm{CBZ}] = (k_d + k_{\cdot OH,CBZ}[^{\bullet}\mathrm{OH}]_{ss})[\mathrm{CBZ}] \quad \text{(S9)}$$

$$-\frac{\mathrm{d[IBP]}}{\mathrm{dt}} = k^{s}_{obs,IBP}[\mathrm{IBP}] = k_d([\mathrm{IBP^0}]+[\mathrm{IBP^-}]) + k_{\cdot OH,IBP^0}[^{\bullet}\mathrm{OH}]_{ss}[\mathrm{IBP^0}] + k_{\cdot OH,IBP^-}[^{\bullet}\mathrm{OH}]_{ss}[\mathrm{IBP^-}] \quad \text{(S10)}$$

$$-\frac{\mathrm{d[NAP]}}{\mathrm{dt}} = k^{s}_{obs,NAP}[\mathrm{NAP}] = k_d([\mathrm{NAP^0}]+[\mathrm{NAP^-}]) + k_{\cdot OH,NAP^0}[^{\bullet}\mathrm{OH}]_{ss}[\mathrm{NAP^0}] + k_{\cdot OH,NAP^-}[^{\bullet}\mathrm{OH}]_{ss}[\mathrm{NAP^-}] + \sum_i k_{i,NAP^0}[x_i][\mathrm{NAP^0}] + \sum_i k_{i,NAP^-}[x_i][\mathrm{NAP^-}] \quad \text{(S11)}$$

where $k^{s}_{obs,CBZ}$, $k^{s}_{obs,IBP}$, $k^{s}_{obs,NAP}$ are the overall pseudo-first-order rate constants of CBZ, IBP and NAP degradation, respectively. $k_{\cdot OH,CBZ}$, $k_{\cdot OH,IBP0}$, $k_{\cdot OH,IBP-}$, $k_{\cdot OH,NAP0}$ and $k_{\cdot OH,NAP-}$ are the second-order rate constants of CBZ, IBP^0, IBP^-, NAP^0 and NAP^- with $^{\bullet}OH$. The x_i represents all radicals generated from the UV/PAA process except $^{\bullet}OH$. $k_{xi,NAP0}$ and $k_{xi,NAP-}$ are the second-order rate constants of other radicals with NAP. The contributions of other potential radicals generated from UV/PAA were neglected, due to the lack of second-order rate constants of them with NAP. Therefore, Eq.S11 can be simplified as follows:

$$-\frac{\mathrm{d[NAP]}}{\mathrm{dt}} = k_d([\mathrm{NAP^0}]+[\mathrm{NAP^-}]) + k_{\cdot OH,NAP^0}[^{\bullet}\mathrm{OH}]_{ss}[\mathrm{NAP^0}] + k_{\cdot OH,NAP^-}[^{\bullet}\mathrm{OH}]_{ss}[\mathrm{NAP^-}] \quad \text{(S12)}$$

The values of $k_{\cdot OH,CBZ}$, $k_{\cdot OH,IBP-}$ and $k_{\cdot OH,NAP-}$ are known in the literature[12-14] and listed in Table S2. The values of $k_{\cdot OH,IBP0}$ and $k_{\cdot OH,NAP0}$ were determined by competition kinetic method using NB as a competitor[4-8] (described in Text S4) to be 9.49×10^9 $M^{-1}\cdot s^{-1}$ and 1.69×10^{10} $M^{-1}\cdot s^{-1}$, respectively. With these calculated and known rate constants and the calculated $[^{\bullet}OH]_{ss}$, $k^{s}_{obs,CBZ}$, $k^{s}_{obs,IBP}$, $k^{s}_{obs,NAP}$ could be obtained to predict the degradation of CBA, IBP and NAP in the UV/PAA process.

Text S7. Identification of Products of CBA, IBP and NAP by UV/PAA and UV/H_2O_2

To evaluate the transformation products of pharmaceuticals by UV/PAA, experiments were conducted with higher concentrations (4×) of PAA and target compound and without adding buffer to control pH (40 mg/L PAA, 40 μM pharmaceutical, pH 3.30). For comparison, product analysis was also conducted for experiments under UV/H_2O_2 and the solution pH was adjusted to 3.17 by $HClO_4$. The H_2O_2 dosage (22.5 mg/L, i.e., 0.66 mM) for UV/H_2O_2 was equal to the sum of PAA (0.53 mM) and H_2O_2 (0.13 mM) concentrations in PAA solution. Sample aliquots were taken at different reaction times and analyzed immediately by LC/MS.

Transformation products of CBZ. Seventeen new peaks considered as products of CBZ were observed in the UV/PAA experiment (Table S3), and ten of them (*m/z* of 269c, 271d, 287, 267, 253a, 269d, 242, 253b, 253c and 226) having significant peaks may be the major transformation products. The ion fragments of some products were proposed according to the MS spectra under 220 eV fragmentation voltage (Table S3). In the UV/H_2O_2 experiment, eight products were found and seven of them (*m/z* 271d, 287, 253a, 283, 253b, 253c and 226)

were detected in the UV/PAA process except for *m/z* 251. Assuming similar MS signal response for each product, the most abundant products (*m/z* 253a, 253b and 226) were the same in both conditions, indicating the mechanisms of CBZ degradation under UV/PAA and UV/H_2O_2 were similar, primarily due to $^{\bullet}OH$. According to the peak area evolution of each product, all products were transient intermediates and the amount of products (peak areas) were lower under UV/H_2O_2 than under UV/PAA (Figure S6), which may be due to faster degradation of these products under the employed UV/H_2O_2 conditions.

The proposed structures of CBZ transformation products are presented in Figure S7. Among them, *m/z* 253a-c have the same fragment ion at *m/z* 210 (-43), which could correspond to CONH loss. The +16 mass increase compared with CBZ indicated that *m/z* 253a-c could be monohydroxylated, epoxide or oxygenous derivatives of CBZ. The structures of *m/z* 253 products were also proposed in the degradation of CBZ by chlorination, UV/H_2O_2, UV/Fe(II), PMS/Co^{II} or hydrodynamic-acoustic cavitation processes.[23-26] The *m/z* 271a-d showed a +34 mass increase compared with CBZ, and the observed fragment ions at *m/z* 253 (-18) and 210 (-43) could correspond to H_2O and CONH loss. Thus, *m/z* 271a-d could be the diol derivatives of CBZ with olefinic double bond opening, in which 10,11-dihydroxycarbbamazepine was mentioned in previous studies.[23,24,26] The *m/z* 269a-d with +32 mass increase from *m/z* 237 could be dihydroxy-CBZ isomers generated by hydroxylation on the aromatic ring, which were proposed previously.[27,28] Moreover, one of *m/z* 269a-d may be diketone derivatives of CBZ formed by breaking the double bone on CBZ. The *m/z* 267 product was likely similar to that detected in CBZ degradation by Fe(VI).[29] For *m/z* 226, two fragment ions at *m/z* 208 and 180 arose from the loss of H_2O and CO, and the proposed structure here was in accordance with previous studies about CBZ degradation by UV, UV/H_2O_2 or simulated solar irradiation.[27,30,31] The *m/z* 251 detected under UV/H_2O_2 was identified as a quinonid derivative of CBZ proposed in previous research.[28]

Additionally, several new products (*m/z* 287, 283, 242 and 138) not identified before were detected in this study. The *m/z* 287 with +16 mass increase from *m/z* 271 had the same fragment ion at *m/z* 210 and 180 with *m/z* 253a, 271b and 271d, indicating that *m/z* 287 may be the triol derivative of CBZ with olefinic double bond opening. The *m/z* 283 with +46 mass increase from CBZ had a fragment ion of *m/z* 265(-18) with H_2O loss, indicating the presence of a hydroxyl group and thus additional CH_2O was added on CBZ. The *m/z* 242 had the fragment ions at *m/z* 214(-18) and 196(-36) which could arise from one to two H_2O loss, suggesting *m/z* 242 may have two hydroxyl groups. Considering the +5 mass increase compared with CBZ, the *m/z* 242 formed from diol-CBZ should lose 27 Dalton, which could correspond to CHN loss. To further verify the proposed structures for these new products, MS/MS information or other identification methods are needed.

Transformation products of IBP. In both UV/PAA and UV/H_2O_2 experiments, eleven products were tentatively identified and eight of them (*m/z* 205a, 203, 205b, 205c, 223, 161,

177a and 177b) showed high peak areas and could be the major transformation products (Table S4). From product evolution, the most abundant products were different for UV/PAA and UV/H_2O_2 (Figure S8). Under UV/PAA, *m/z* 161, 203 and 177b were the dominant products while *m/z* 233 and 203 were most abundant under UV/H_2O_2. Similar to CBZ experiments, the peak areas of IBP products under UV/PAA were higher than that under UV/H_2O_2 due to the different degradation rates.

The structures of transformation products are proposed in Figure S9. Compared to IBP, *m/z* 223 with +16 mass increase could be monohydroxylated IBP. Decarboxylation of IBP may form *m/z* 161. The *m/z* 177a,b could be generated by decarboxylation and deprotonation after hydroxylation of *m/z* 161. Additionally, *m/z* 177a,b could be hydroxylated to produce *m/z* 193a,b.[32-34] The IBP transformation products with *m/z* 177, 223 and 193 have been reported in other $^{\bullet}$OH-induced AOPs (e.g., photo-Fenton, TiO_2 photocatalysis, electro-peroxone process and gamma irradiation).[32-37] Moreover, the *m/z* 203 and 205a-d products were not detected previously and more advanced analytical techniques are needed to identify their structures.

Transformation products of NAP. Thirty-three products of NAP degradation were found under UV/PAA and twenty-seven of them were detected in the UV/H_2O_2 experiment (Table S5). The products of *m/z* 165, 233a, 177, 261a, 233b, 185, 201a and 201b were the major intermediates with significant MS signal responses, in which the *m/z* 185 and 201b were the most abundant products in both UV/PAA and UV/H_2O_2 experiments (Figure S10a,b). Some minor products were only observed under UV/PAA, which were *m/z* 129, 221a, 197, 237, 247a and 247c (Figure S10e). The transformation of NAP by $CH_3CO_2^{\bullet}$ and $CH_3CO_3^{\bullet}$ may be similar to that by $^{\bullet}$OH, based on the similar transformation products under UV/PAA and UV/H_2O_2. Although the NAP degradation was faster under UV/PAA than UV/H_2O_2, higher peak areas were observed for most products under UV/PAA than UV/H_2O_2, suggesting that the selectivity of $CH_3CO_2^{\bullet}$ and $CH_3CO_3^{\bullet}$ to compounds with characteristic structures may lead to more products generated without further degrading them. On the other hand, $^{\bullet}$OH with non-selectivity could attack NAP products to further degrade them and the amount of $^{\bullet}$OH was higher in UV/H_2O_2 than in UV/PAA.

The structures of some products are proposed in Figure 4 in the main paper, according to the information of molecular ions and fragment ions, and previous relevant research. The demethylation of methoxy group, the loss of methoxy group, hydroxylation and dehydration may occur during NAP degradation under UV/PAA. For *m/z* 185, 201b, 203 and 189, the proposed structures are similar to previous studies on NAP degradation by UV, UV/TiO_2, α-MnO_2 nanorods oxidation.[37-41] The main product *m/z* 185 was formed by decarboxylation of NAP, while *m/z* 201b could be generated from oxidation of *m/z* 203 that could be produced by decarboxylation and hydroxylation. The dihydroxylation of *m/z* 201b may produce *m/z* 233a, which can further transform into a quinone derivative m/z 231b. The *m/z* 247a-d could

be hydroxylated NAP isomers considering +16 mass increase from NAP. Except for *m/z* 185, 201b, 203 and 189, only twelve of NAP degradation products were provided with tentative structures due to the limited information. To confirm the specific structures of these products, more advanced analytical techniques are needed.

Table S1. Contributions of ·OH, Carbon-Centered Radicals and Direct Photolysis to the Degradation of NAP and Substructure Compounds under UV/PAA at pH 7.10

Pharmaceuticals	·OH	Carbon-centered radicals	Direct photolysis	k_{obs} (min^{-1})
NAP	49.9%	34.1%	16.0%	$(3.07\pm0.07)\times10^{-1}$
NP	84.1%	6.1%	9.7%	$(1.19\pm0.04)\times10^{-1}$
AS	82.2%	3.0%	14.8%	$(8.41\pm0.31)\times10^{-2}$
2-NPAA	57.4%	31.5%	11.1%	$(7.02\pm0.30)\times10^{-2}$

Table S2. Reactions in UV/PAA System

Reaction	Rate constant	Reference
$PAA^0 \Leftrightarrow PAA^- + H^+$	$pK_a = 8.20$	15
$H_2O_2 \Leftrightarrow HO_2^- + H^+$	$pK_a = 11.6$	16
$HAc \Leftrightarrow Ac^- + H^+$	$pK_a = 4.76$	17
$IBP^0 \Leftrightarrow IBP^- + H^+$	$pK_a = 4.91$	18
$NAP^0 \Leftrightarrow NAP^- + H^+$	$pK_a = 4.15$	18
$H_2CO_3 \Leftrightarrow HCO_3^- + H^+ \Leftrightarrow CO_3^{2-} + 2H^+$	$pK_{a1} = 6.3$, $pK_{a2} = 10.3$	19
$PAA^0 + {}^{\bullet}OH \rightarrow$ products	$9.33\times10^8\ M^{-1}\cdot s^{-1}$	This study
$PAA^- + {}^{\bullet}OH \rightarrow$ products	$9.97\times10^9\ M^{-1}\cdot s^{-1}$	This study
$H_2O_2 + {}^{\bullet}OH \rightarrow HO_2^{\bullet} + H_2O$	$2.7\times10^7\ M^{-1}\cdot s^{-1}$	11
$HO_2^- + {}^{\bullet}OH \rightarrow HO_2^{\bullet} + OH^-$	$7.5\times10^9\ M^{-1}\cdot s^{-1}$	20
$CO_3^{2-} + {}^{\bullet}OH \rightarrow CO_3^{\bullet-} + OH^-$	$3.9\times10^8\ M^{-1}\cdot s^{-1}$	11
$HCO_3^- + {}^{\bullet}OH \rightarrow CO_3^{\bullet-} + H_2O$	$8.5\times10^6\ M^{-1}\cdot s^{-1}$	11
CH_3CO_2H (HAc) $+ {}^{\bullet}OH \rightarrow {}^{\bullet}CH_2CO_2H + H_2O$	$9.2\times10^6\ M^{-1}\cdot s^{-1}$	21
$CH_3CO_2^-$ (Ac^-) $+ {}^{\bullet}OH \rightarrow {}^{\bullet}CH_2CO_2^- + H_2O$	$8.5\times10^7\ M^{-1}\cdot s^{-1}$	22
CBZ $+ {}^{\bullet}OH \rightarrow$ products	$8.8\times10^9\ M^{-1}\cdot s^{-1}$	12
$IBP^0 + {}^{\bullet}OH \rightarrow$ products	$9.49\times10^9\ M^{-1}\cdot s^{-1}$	This study
$IBP^- + {}^{\bullet}OH \rightarrow$ products	$7.04\times10^9\ M^{-1}\cdot s^{-1}$	13
$NAP^0 + {}^{\bullet}OH \rightarrow$ products	$1.69\times10^{10}\ M^{-1}\cdot s^{-1}$	This study
$NAP^- + {}^{\bullet}OH \rightarrow$ products	$8.61\times10^9\ M^{-1}\cdot s^{-1}$	14

Table S3. The LC/MS Analysis of CBZ and Its Transformation Products

$[M+H]^+$	Ion fragments (m/z) detected at 220 eV	Retention time (min)	The detected Condition
237 (CBZ)	194 (-NHCO)	50.3	-
271a	-	15.1	UV/PAA
138	-	14.8	UV/PAA
271b	210, 180	21.5	UV/PAA
269a	226, 180	27.7	UV/PAA
269b	226, 210, 170	30.9	UV/PAA
271c	253, 210	33.9	UV/PAA
269c	208	37.2	UV/PAA
271d	253, 210, 180	37.5	UV/PAA, UV/H_2O_2
287	236, 210, 180	38.2	UV/PAA, UV/H_2O_2
267	196	38.5	UV/PAA
253a	210, 180	39.9	UV/PAA, UV/H_2O_2
269d	-	40.2	UV/PAA
251	-	41.9	UV/H_2O_2
283	265, 222	41.1	UV/PAA, UV/H_2O_2
242	214, 196	42.2	UV/PAA
253b	210	44.1	UV/PAA, UV/H_2O_2
253c	210	45.9	UV/PAA, UV/H_2O_2
226	208, 180	57.5	UV/PAA, UV/H_2O_2

* Products underlined showed large peak areas and could be major products.

Table S4. The LC/MS Analysis of IBP and Its Transformation Products

$[M+H]^+$	Ion Fragments (m/z) detected at 140 eV	Retention time (min)	The detected Condition
207 (IBP)	161	50.8	-
193a	-	27.2	UV/PAA, UV/H_2O_2
205a	163	28.0	UV/PAA, UV/H_2O_2
203	177, 157	29.0	UV/PAA, UV/H_2O_2
205b	163	30.4	UV/PAA, UV/H_2O_2
205c	-	31.6	UV/PAA, UV/H_2O_2
205d	-	33.5	UV/PAA, UV/H_2O_2
223	177	41.6	UV/PAA, UV/H_2O_2
193b	-	41.9	UV/PAA, UV/H_2O_2
161	119	47.5	UV/PAA, UV/H_2O_2
177a	-	48.2	UV/PAA, UV/H_2O_2
177b	-	49.3	UV/PAA, UV/H_2O_2

* Products underlined showed large peak areas and could be major products.

Table S5. The LC/MS Analysis of NAP and Its Transformation Products

$[M+H]^+$	Ion Fragments (m/z) detected at 150 eV	Retention time (min)	The detected Condition
231a (NAP)	185	44.7	-
143		2.6	UV/PAA, UV/H_2O_2
129		2.5	UV/PAA
189		2.4	UV/PAA, UV/H_2O_2
203a		2.5	UV/PAA, UV/H_2O_2
211	193	3.4	UV/PAA, UV/H_2O_2
209	191	4.2	UV/PAA, UV/H_2O_2
179		4.7	UV/PAA, UV/H_2O_2
249a		4.6	UV/PAA, UV/H_2O_2
221a		4.8	UV/PAA
265		5.5	UV/PAA, UV/H_2O_2
205a		5.6	UV/PAA, UV/H_2O_2
197	179	5.5	UV/PAA
237		5.9	UV/PAA
203b		6.2	UV/PAA, UV/H_2O_2
249b		7.8	UV/PAA, UV/H_2O_2
<u>165</u>		8.5	UV/PAA, UV/H_2O_2
<u>233a</u>		12.0	UV/PAA, UV/H_2O_2
205b		12.6	UV/PAA, UV/H_2O_2
<u>177</u>		14.8	UV/PAA, UV/H_2O_2
285		16.6	UV/PAA, UV/H_2O_2
231b		16.5	UV/PAA, UV/H_2O_2
221b		17.0	UV/PAA, UV/H_2O_2
<u>261a</u>		17.7	UV/PAA, UV/H_2O_2
247a		17.9	UV/PAA
247b	201	22.2	UV/PAA, UV/H_2O_2
221c		22.7	UV/PAA, UV/H_2O_2
247c	201	23.5	UV/PAA
<u>233b</u>	215	25.8	UV/PAA, UV/H_2O_2
261b	215	27.9	UV/PAA, UV/H_2O_2
247d		31.3	UV/PAA, UV/H_2O_2
<u>185</u>		34.0	UV/PAA, UV/H_2O_2
<u>201a</u>	185	37.0	UV/PAA, UV/H_2O_2
<u>201b</u>		44.6	UV/PAA, UV/H_2O_2

* Products underlined showed large peak areas and could be major products.

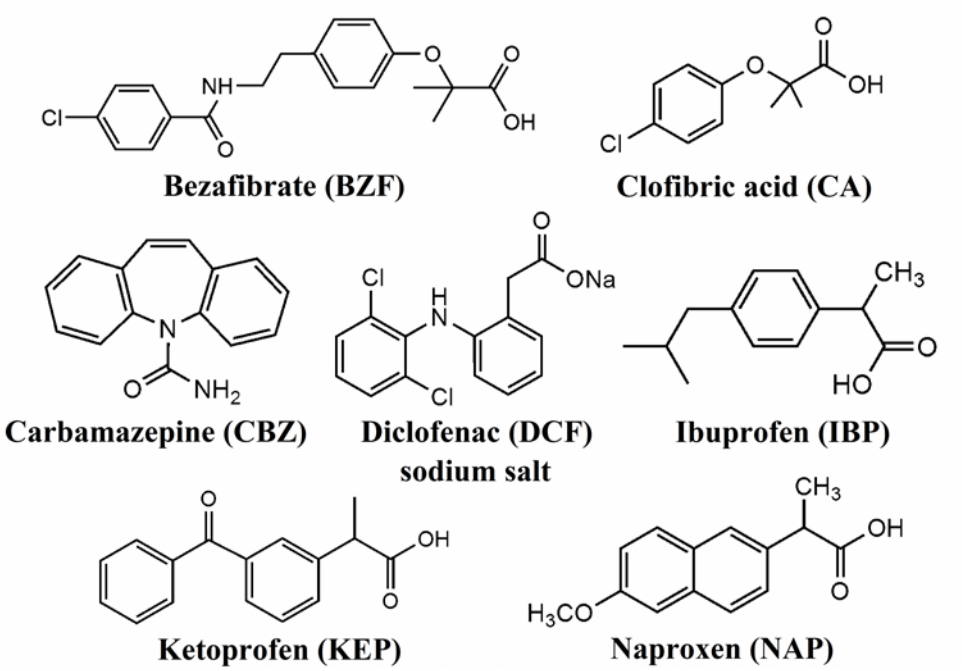

Figure S1. Structures of target pharmaceuticals.

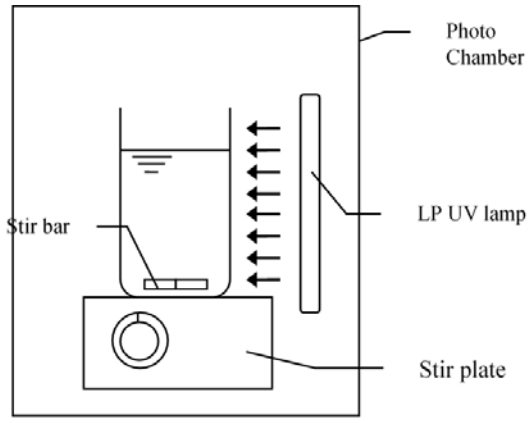

Figure S2. Illustrations of photolysis experimental setup. An air fan in the back of the photo-chamber was turned on during the experiments for cooling and a circular hole with cover in the top of the photo-chamber was used for adding oxidants or sampling.

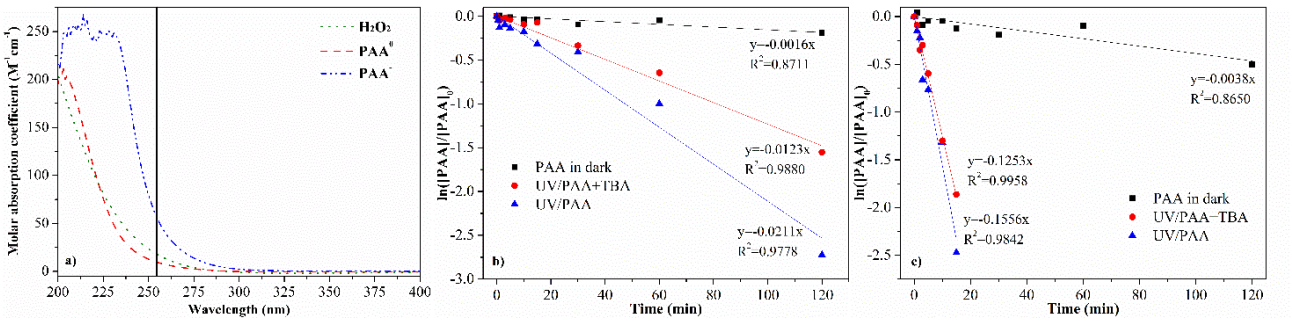

Figure S3. The molar absorption coefficients (a) of PAA^0, PAA^- and H_2O_2 across 200-400 nm at 25 ± 1 °C and photolysis of PAA (1 mg/L，i.e., 13.1 μM) under UV or UV+TBA at (b) pH 5.09; and (c) pH 9.65.

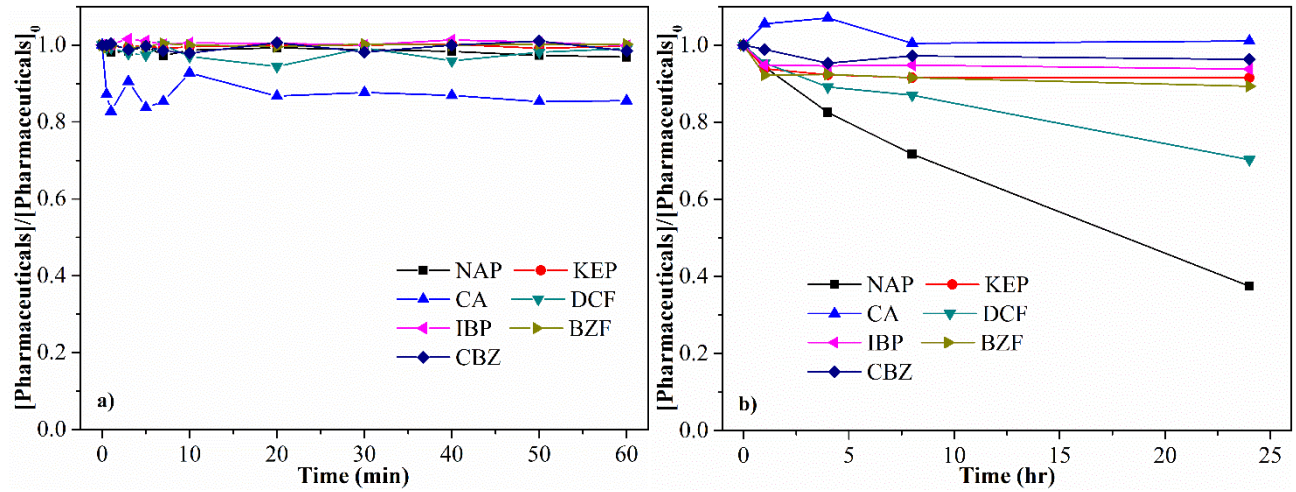

Figure S4. The degradation of pharmaceuticals under PAA alone: a) 1 mg/L PAA dosage, pH 7.10; b) 1 g/L PAA dosage, pH 3.18. Initial pharmaceutical concentration was 1 μM.

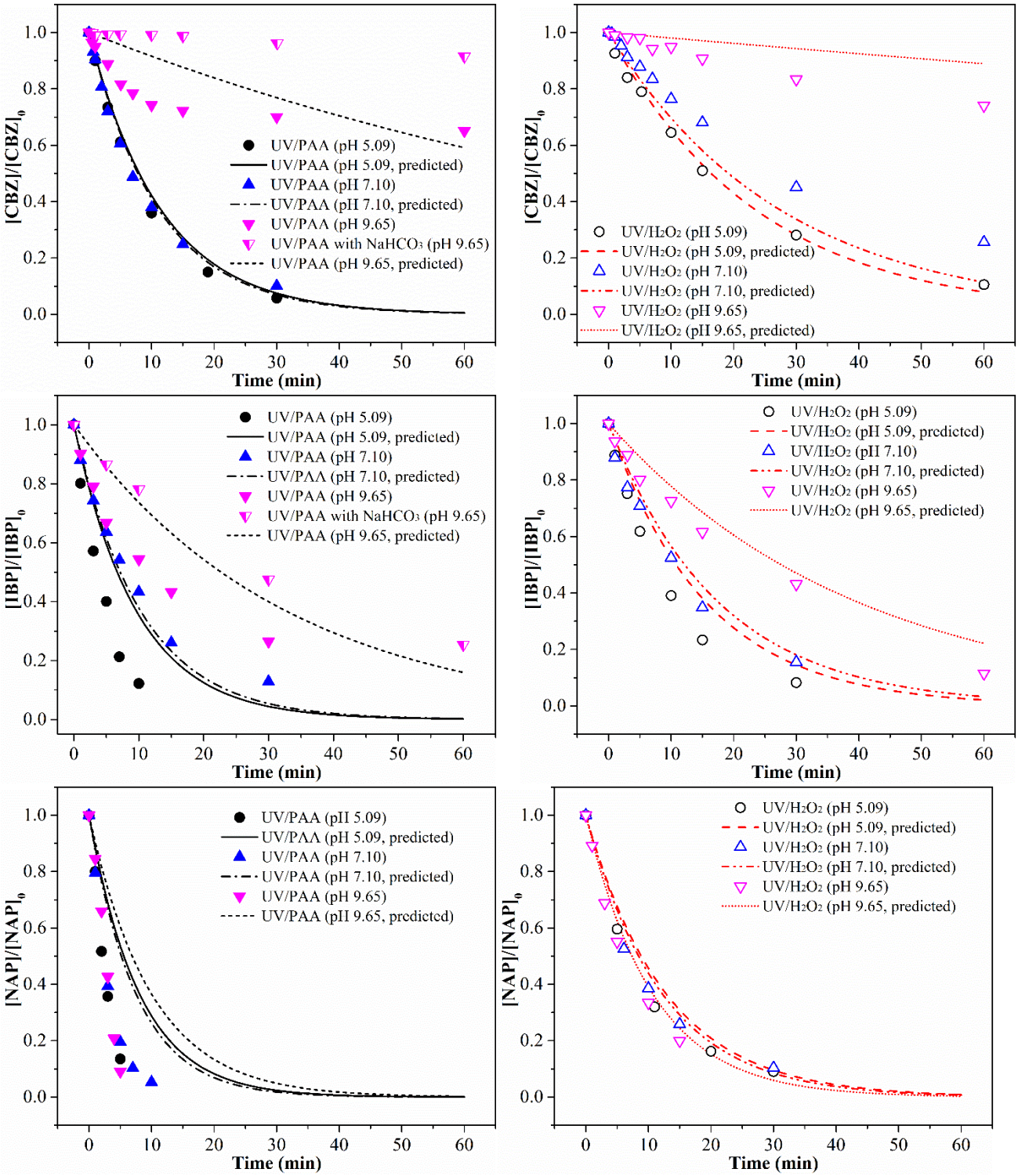

Figure S5. The predicted and experimental degradation of CBZ, IBP and NAP under UV/PAA (left) and UV/H_2O_2 (right) at different pH by considering the contributions of $^{\bullet}OH$ and direct photolysis. Experimental conditions: $[pharmaceutical]_0$ = 1 μM, $[PAA]_0$ = 1 mg/L, $[H_2O_2]_0$ = 0.11±0.01 mg/L, $[NaHCO_3]_0$ = 25.9 mM, [buffer] = 10 mM, 25 °C.

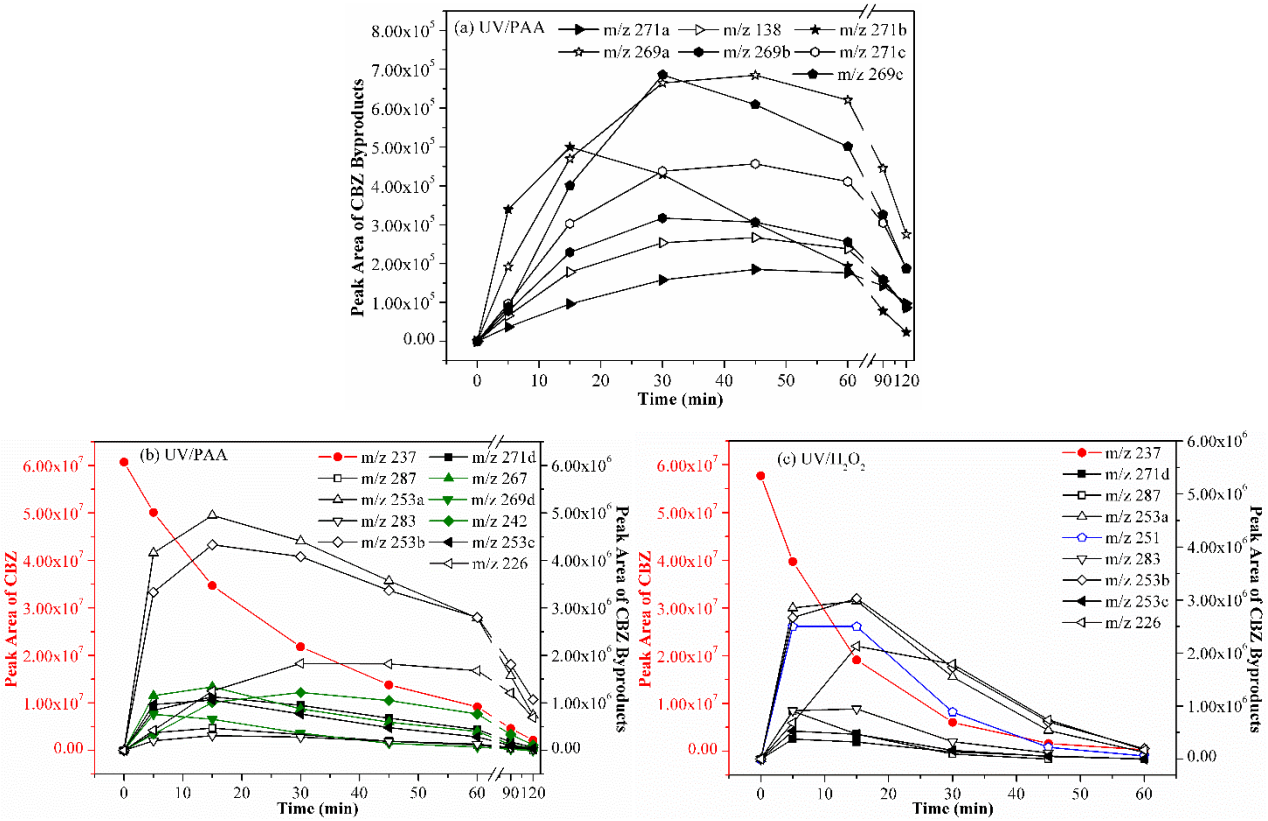

Figure S6. Degradation products of CBZ under UV/PAA and UV/H_2O_2. Reaction condition: $[PAA]_0$ = 40 mg/L, $[H_2O_2]_0$ = 22.5 mg/L, $[CBZ]_0$ = 40 μM.

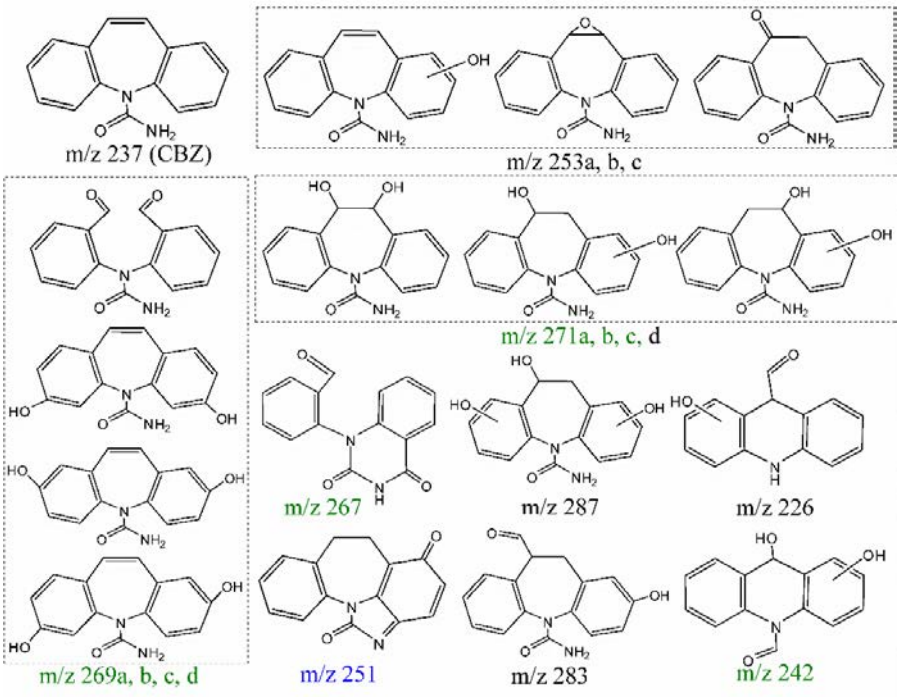

Figure S7. Structures of CBZ and proposed transformation products.

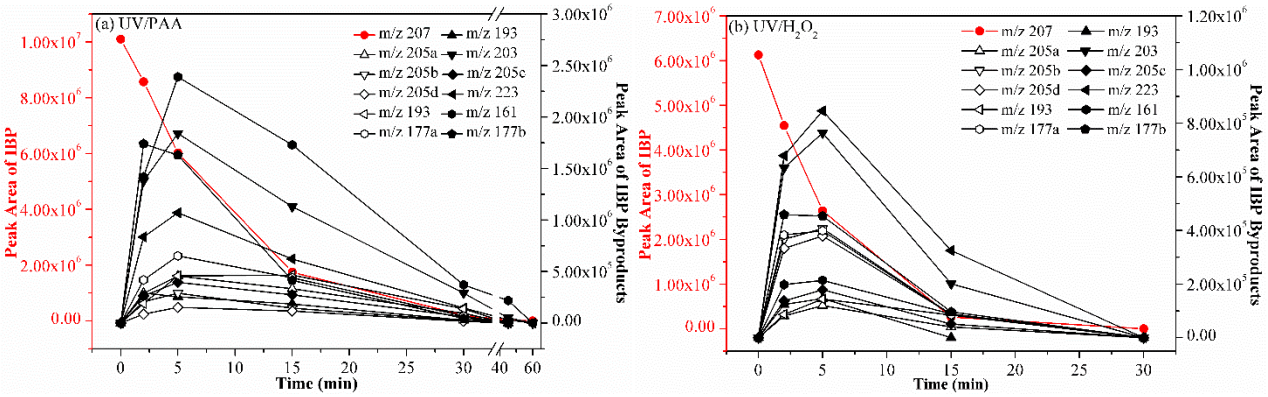

Figure S8. Degradation products of IBP under UV/PAA and UV/H_2O_2. Reaction condition: $[PAA]_0$ = 40 mg/L, $[H_2O_2]_0$ = 22.5 mg/L, $[IBP]_0$ = 40 μM.

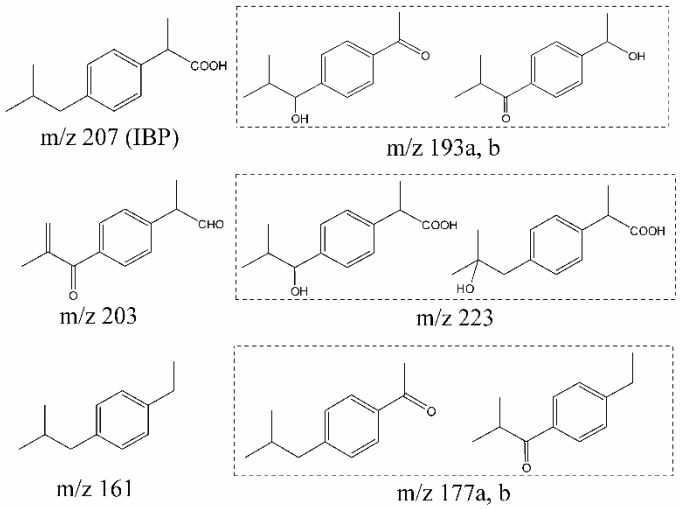

Figure S9. Structures of IBP and proposed transformation products.

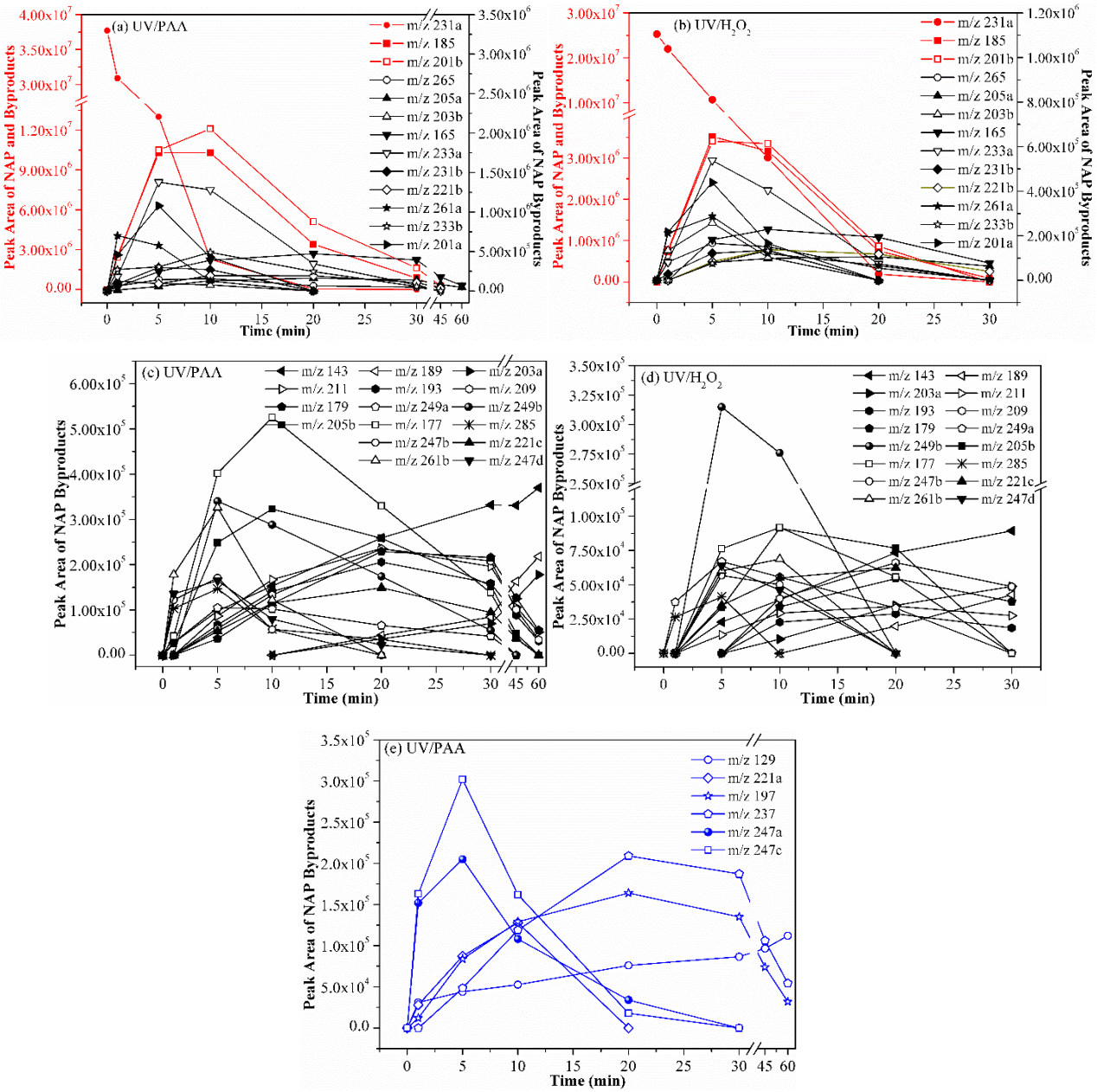

Figure S10. Degradation products of NAP under UV/PAA and UV/H_2O_2. Reaction condition: $[PAA]_0$ = 40.0 mg/L, $[H_2O_2]_0$ = 22.5 mg/L, $[NAP]_0$ = 40 μM.

References

(1) Block, S. S. Peroxygen compounds. In *Disinfection, Sterilization, and Preservation*, 5th ed.; Block, S. S., Ed.; Pa, Philadelphia 1991; pp 185-205.

(2) Kitis, M. Disinfection of wastewater with peracetic acid: a review. *Environ. Int.* **2004**, *30* (1), 47-55.

(3) APHA-AWWA-WEF. *Standard Methods for the Examination of Water and Wastewater*, 20th ed.; American Public Health Association/American Water Works Association/Water Environment Federation: Washington DC, 1998.

(4) Zhang, R.; Sun, P.; Boyer, T. H.; Zhao, L.; Huang, C. H. Degradation of pharmaceuticals and metabolite in synthetic human urine by UV, UV/H_2O_2, and UV/PDS. *Environ. Sci. Technol.* **2015**, *49* (5), 3056-3066.

(5) Fang, J.; Fu, Y.; Shang, C. The roles of reactive species in micropollutant degradation in the UV/free chlorine system. *Environ. Sci. Technol.* **2014**, *48* (3), 1859-1868.

(6) Yuan, F.; Hu, C.; Hu, X.; Qu, J.; Yang, M. Degradation of selected pharmaceuticals in aqueous solution with UV and UV/H_2O_2. *Water Res.* **2009**, *43* (6), 1766-1774.

(7) Onstein, P.; Stefan, M. I.; Bolton, J. R. Competition kinetics method for the determination of rate constants for the reaction of hydroxyl radicals with organic pollutants. *J. Adv. Oxid. Technol.* **1999**, *4* (2), 231-236.

(8) Pereira, V. J.; Weinberg, H. S.; Linden, K. G.; Singer, P. C. UV Degradation Kinetics and Modeling of Pharmaceutical Compounds in Laboratory Grade and Surface Water via Direct and Indirect Photolysis at 254 nm. *Environ. Sci. Technol.* **2007**, *41* (5), 1682-1688.

(9) Elovitz, M. S.; von Gunten, U. Hydroxyl Radical/Ozone Ratios During Ozonation Processes. I. *The Rct Concept. Ozone Sci. Eng.* **1999**, *21* (3), 239-260.

(10) Zepp, R. G.; Hoigne, J.; Bader, H. Nitrate-induced photooxidation of trace organic chemicals in water. *Environ. Sci. Technol.* **1987**, *21* (5), 443-450.

(11) Buxton, G. V.; Greenstock, C. L.; Helman, W. P.; Ross, A. B. Critical Review of Rate Constants for Reactions of Hydrated Electrons, Hydrogen Atoms and Hydroxyl Radicals ($^{\bullet}OH/^{\bullet}O^-$) in Aqueous solution. *J. Phys. Chem. Ref. Data.* **1988**, *17* (2), 513-886.

(12) Huber, M. M.; Canonica, S.; Park, G.-Y.; von Gunten, U. Oxidation of Pharmaceuticals during Ozonation and Advanced Oxidation Processes. *Environ. Sci. Technol.* **2003**, *37* (5), 1016-1024.

(13) Wols, B. A.; Hofman-Caris, C. H. Review of photochemical reaction constants of organic micropollutants required for UV advanced oxidation processes in water. *Water Res.* **2012**, *46* (9), 2815-2827.

(14) Huber, M. M.; GÖbel, A.; Joss, A.; Hermann, N.; LÖffler, D.; McArdell, C. S.; Ried, A.; Siegrist, H.; Ternes, T. A.; von Gunten, U. Oxidation of Pharmaceuticals during Ozonation of Municipal Wastewater Effluents: A Pilot Study. *Environ. Sci. Technol.* **2005**, *39* (11), 4290-4299.

(15) Wagner, M.; Brumelis, D.; Gehr, R. Disinfection of Wastewater by Hydrogen Peroxide or Peracetic Acid: Development of Procedures for Measurement of Residual Disinfectant and Application to a Physicochemically Treated Municipal Effluent. *Water Environ. Res.* **2002**, *74* (1), 33-50.

(16) Perry, R. H.; Green, D. W.; Maloney, J. D. Chemical Engineer's Handbook 5th edn. **1981**, McGraw-Hill, New York.

(17) Goldberg, R. N.; Kishore, N.; Lennen, R. M. Thermodynamic Quantities for the Ionization Reactions of Buffers. *J. Phys. Chem. Ref. Data.* **2002**, *31* (2), 231-370.

(18) Packer, J.; Werner, J. J.; Latch, D.E.; McNeill, K.; Arnold, W.A. Photochemical fate of pharmaceuticals in the environment: Naproxen, diclofenac, clofibric acid, and ibuprofen. *Aquat. Sci.* **2003**, *65* (4), 342-351.

(19) Stumm, W.; Morgan, J. J. *Aquatic Chemistry* (3rd); Wiley-Interscience: New York, USA, **1996**.

(20) Christensen, H. S.; Sehested, K.; Corftizan, H. Reaction of hydroxyl radicals with hydrogen peroxide at ambient temperatures. *J. Phys. Chem.* **1982**, *86*, 15-88.

(21) Thomas, J. K. "Rates of reaction of the hydroxyl radical." *Trans. Faraday Soc.* **1965**, *81* (61), 133-140.

(22) Willson, R. L.; Greenstock, C.L.; Adams, G. E.; Wageman, R.; Dorfman, L. M. "The standardization of hydroxyl radical rate data from radiation chemistry." *Int. J. Radiat. Phys. Chem.* **1971**, *3* (3), 211-220.

(23) Braeutigam, P.; Franke, M.; Schneider, R. J.; Lehmann, A.; Stolle, A.; Ondruschka, B. Degradation of carbamazepine in environmentally relevant concentrations in water by Hydrodynamic-Acoustic-Cavitation (HAC). *Water Res.* **2012**, *46* (7), 2469-2477.

(24) Liu, N.; Zheng, M.; Sijak, S.; Tang, L.; Xu, G.; Wu, M. Aquatic photolysis of carbamazepine by UV/H_2O_2 and UV/Fe(II) processes. *Res. Chem. Intermed.* **2014**, *41* (10), 7015-7028.

(25) Matta, R.; Tlili, S.; Chiron, S.; Barbati, S. Removal of carbamazepine from urban wastewater by sulfate radical oxidation. *Environ. Chem. Lett.* **2010**, *9* (3), 347-353.

(26) Soufan, M.; Deborde, M.; Delmont, A.; Legube, B. Aqueous chlorination of carbamazepine: kinetic study and transformation product identification. *Water Res.* **2013**, *47* (14), 5076-5087.

(27) Calisto, V.; Domingues, M. R.; Erny, G. L.; Esteves, V. I. Direct photodegradation of carbamazepine followed by micellar electrokinetic chromatography and mass spectrometry. *Water Res.* **2011**, *45* (3), 1095-1104.

(28) Chiron, S.; Minero, C.; Vione, D. Photodegradation processes of the antiepileptic drug carbamazepine, relevant to estuarine waters. *Environ. Sci. Technol.* **2006**, *40* (19), 5977-5983.

(29) Zhou, Z.; Jiang, J. Q. Treatment of selected pharmaceuticals by ferrate(VI): performance, kinetic studies and identification of oxidation products. *J. Pharm. Biomed. Anal.* **2015**, *106*, 37-45.

(30) Kosjek, T.; Andersen, H. R.; Kompare, B.; Ledin, A.; Heath, E. Fate of carbamazepine during water treatment. *Environ. Sci. Technol.* **2009**, *43* (16), 6256-6261.

(31) Lekkerkerker-Teunissen, K.; Benotti, M. J.; Snyder, S. A.; van Dijk, H. C. Transformation of atrazine, carbamazepine, diclofenac and sulfamethoxazole by low and medium pressure UV and UV/H_2O_2 treatment. *Sep. Purif. Technol.* **2012**, *96*, 33-43.

(32) Li, X.; Wang, Y.; Yuan, S.; Li, Z.; Wang, B.; Huang, J.; Deng, S.; Yu, G. Degradation of the anti-inflammatory drug ibuprofen by electro-peroxone process. *Water Res.* **2014**, *63*, 81-93.

(33) Madhavan, J.; Grieser, F.; Ashokkumar, M. Combined advanced oxidation processes for the synergistic degradation of ibuprofen in aqueous environments. *J. Hazard. Mater.* **2010**, *178* (1-3), 202-208.

(34) Mendez-Arriaga, F.; Esplugas, S.; Gimenez, J. Degradation of the emerging contaminant ibuprofen in water by photo-Fenton. *Water Res.* **2010**, *44* (2), 589-595.

(35) Zheng, B. G.; Zheng, Z.; Zhang, J. B.; Luo, X. Z.; Wang, J. Q.; Liu, Q.; Wang, L. H. Degradation of the emerging contaminant ibuprofen in aqueous solution by gamma irradiation. *Desalination* **2011**, *276* (1-3), 379-385.

(36) Illes, E.; Takacs, E.; Dombi, A.; Gajda-Schrantz, K.; Racz, G.; Gonter, K.; Wojnarovits, L. Hydroxyl radical induced degradation of ibuprofen. *Sci. Total Environ.* **2013**, *447*, 286-292.

(37) Arany, E.; Szabo, R. K.; Apati, L.; Alapi, T.; Ilisz, I.; Mazellier, P.; Dombi, A.; Gajda-Schrantz, K. Degradation of naproxen by UV, VUV photolysis and their combination. *J. Hazard. Mater.* **2013**, *262*, 151-157.

(38) Jallouli, N.; Elghniji, K.; Hentati, O.; Ribeiro, A. R.; Silva, A. M.; Ksibi, M. UV and solar photo-degradation of naproxen: TiO_2 catalyst effect, reaction kinetics, products identification and toxicity assessment. *J. Hazard. Mater.* **2016**, *304*, 329-336.

(39) Kanakaraju, D.; Motti, C. A.; Glass, B. D.; Oelgemoller, M. TiO_2 photocatalysis of naproxen: effect of the water matrix, anions and diclofenac on degradation rates. *Chemosphere* **2015**, *139*, 579-588.

(40) Marotta, R.; Spasiano, D.; Di Somma, I.; Andreozzi, R. Photodegradation of naproxen and its photoproducts in aqueous solution at 254 nm: a kinetic investigation. *Water Res.* **2013**, *47* (1), 373-383.

(41) Zhang, Y.; Yang, Y.; Zhang, Y.; Zhang, T.; Ye, M. Heterogeneous oxidation of naproxen in the presence of α-MnO_2 nanostructures with different morphologies. *Appl. Catal. B-Environ.* **2012**, *127*, 182-189.